obtained as large yellow crystals by cooling a saturated toluene solution. Yield = 0.316 g (82%). Anal. Calcd for $Rh_2N_2C_{30}H_{40}$: C, 56.79; H, 6.35; N, 4.41. Found: C, 56.95; H, 6.53; N, 4.67. $^1H$ NMR ($C_6D_6$, 30 °C): δ 2.39 (dd), 4.22 (dd, Rh-C$H_2$-py-6Me); 2.68 (s, 6 *Me*); 3.87 (m), 3.89 (m), 4.06 (m), 4.22 (m, COD-C*H*); 1.8–3.0 (overlapping multiplets, COD-C$H_2$); 5.85 (d), 6.36 (d), 6.56 (t, 3,5,4-*H* of py). $^{13}C$ NMR ($C_6D_6$, 30 °C): δ 10.5 (d, Rh-*C*$H_2$-py-6Me, $^1J(^{103}Rh-^{13}C)$ = 21 Hz); 19.2 (6*Me*); 30.2, 30.9, 32.3, 32.8 (COD-*C*$H_2$); 74.6 (d, $^1J(^{103}Rh-^{13}C)$ = 14 Hz), 75.5 (d, $^1J(^{103}Rh-^{13}C)$ = 15 Hz), 83.1 (d, $^1J(^{103}Rh-^{13}C)$ = 8.6 Hz), 84.1 (d, $^1J(^{103}Rh-^{13}C)$ = 9 Hz) (COD-*C*H).

**[(COD)Ir(μ-CH$_2$-py-6Me-*C*,*N*)]$_2$ (2).** An essentially identical procedure was followed as for **1** only with [(COD)Ir(μ-Cl)]$_2$ (0.20 g, 0.30 mmol) and Li-CH$_2$-py-6Me (0.08 g, 0.65 mmol). Yield of the red crystalline blocks of **2** from toluene = 0.21 g (85%). Anal. Calcd for $Ir_2N_2C_{30}H_{40}$: C, 44.31; H, 4.95; N, 3.44. Found: C, 44.68; H, 5.14; N, 3.36. $^1H$ NMR ($C_6D_6$, 30 °C): δ 3.11 (d), 4.29 (d, Ir-C$H_2$-py-6Me); 2.51 (s, 6 *Me*); 3.10 (m), 3.21 (m), 3.70 (m), 4.11 (m, COD-C*H*); 1.5–3.0 (overlapping multiplets, COD-C$H_2$); 5.79 (d), 6.23 (d), 6.48 (t, 3,5,4-H of py). $^{13}C$ NMR ($C_6D_6$, 30 °C): δ 30.7 (Ir-*C*H$_2$-py-6Me); 24.0 (*Me*); 29.1, 30.0 30.7, 31.5 (COD-*C*H$_2$); 57.4, 60.1, 63.2, 66.1 (COD-*C*H).

**[(COD)Ir(CH$_2$-py-6Me)(PEtPH$_2$)$_2$] (3).** To a solution of **2** (0.12 g, 0.15 mmol) in benzene (10 mL) was added PEtPh$_2$ (0.14 g, 0.65 mmol) in benzene (5 mL). The initially dark red mixture lightened to pale yellow over minutes. Removal of solvent under vacuum yielded a yellow oil, which was taken up in hot hexane. Upon slow cooling of the hexane solution, crystals of **3** were obtained. Yield = 0.22 g (87%). Anal. Calcd for $IrP_2NC_{43}H_{50}$: C, 61.85; H, 6.03; N, 1.67; P, 7.41. Found: C, 61.71; H, 5.95; N, 1.67; P, 7.80. $^1H$ NMR ($C_6D_6$, −20 °C): δ 3.10 (t, Ir-C$H_2$, $^3J(^{31}P-^1H)$ = 10 Hz); 2.20 (s, 6 *Me*); 6.4 (d), 6.5 (d), 6.8 (t, 3,5,4-*H* of py); 1.4–1.9 (overlapping m, COD-C$H_2$); 3.0–3.6 (overlapping m, COD-C*H*).

**[(dppm)Rh(dppm-H)] (4).** A solution of **1** (0.04 g, 0.06 mmol) in benzene (2 mL) was treated with an excess of dppm (0.12 g, 0.30 mmol). Upon warming to 50 °C for 2 min, the initially yellow solution became red, and upon slow cooling, deep-red crystals of the sparingly soluble product were obtained. Yield = 0.10 g (93%). Due to the fact that the crystals obtained contained 2 benzene molecules per Rh and underwent partial solvent loss upon drying, satisfactory elemental analysis was not possible. $^1H$ NMR ($C_6D_6$, 30 °C): δ 3.34 [br, C*H*(PPh$_2$)$_2$], 4.08 [t, C$H_2$(PPh$_2$)$_2$], 6.8–7.9 (m, aromatics). $^{31}P$ NMR ($C_6D_6$, 30 °C): δ −25.8, −20.4 (AA'BB'X patterns due to $^{31}P$ nuclei of dppm and dppm ligands).

**[(dppm)Ir(dppm-H)] (5).** An essentially identical procedure to that used for **4** above only heating the mixture at 80 °C for minutes led to the formation of very sparingly soluble **5**. $^1H$ NMR ($C_6D_6$, 30 °C): δ 3.68 [br, C*H*(PPh$_2$)$_2$], 4.71 [t, C$H_2$(PPh$_2$)$_2$], 6.7–7.0 (m, aromatics).

**Crystallographic Studies.** Crystal data and data collection parameters for compounds **1–4** are contained in Table IV. Further details of the crystallographic study are contained in the supplementary material.

**Acknowledgment.** We thank the National Science Foundation (Grant CHE-8915573) for support of this research.

**Supplementary Material Available:** Tables of fractional coordinates, thermal parameters, and full bond distances and angles for **1–4** (43 pages); tables of observed and calculated structure factors for **1–4** (91 pages). Ordering information is given on any current masthead page.

# Alkylidene-Transfer Processes in the Reactions of Cp$_2$Ta(=CH$_2$)(CH$_3$) with Silanes

Donald H. Berry,*[1] Timothy S. Koloski, and Patrick J. Carroll

*Department of Chemistry and Laboratory for Research on the Structure of Matter, University of Pennsylvania, Philadelphia, Pennsylvania 19104-6323*

*Received May 7, 1990*

Cp$_2$Ta(=CH$_2$)(Me) (**1**; Cp ≡ η$^5$-C$_5$H$_5$) reacts with relatively unhindered silanes such as Me$_2$SiH$_2$ and Me$_3$SiH in tetrahydrofuran (THF) or benzene to produce equal amounts of Cp$_2$Ta(H$_2$C=CH$_2$)(Me) and the bis(silyl) complexes Cp$_2$Ta(SiR$_3$)$_2$(H) (SiR$_3$ = SiMe$_2$H, SiMe$_3$) with concurrent liberation of methane. The reaction mechanism involves rate-limiting disproportionation of **1** to Cp$_2$Ta(H$_2$C=CH$_2$)(Me) and the unsaturated intermediate Cp$_2$Ta(Me), which subsequently reacts with silanes to yield the bis(silyl) complexes. In contrast, **1** reacts with the hindered silane H$_2$Si(*t*-Bu)$_2$ in THF to yield the silyl-substituted alkylidene hydride complex Cp$_2$Ta(H)(=C(H)(SiH(*t*-Bu)$_2$)) (**2**) and varying amounts of the bridging alkylidene complex {CpTa(μ$_2$-η$^1$:η$^5$-C$_5$H$_4$)}$_2$(μ-C(H)(SiH(*t*-Bu)$_2$)) (**3**). In this instance, the reaction proceeds by a novel chain mechanism involving alkylidene transfer between tantalum centers in which the key chain-carrying species is the unsaturated intermediate Cp$_2$Ta(Me). Reversible hydrogen transfer from tantalum to the alkylidene carbon in **2** is facile, and the resultant unsaturated alkyl can be readily trapped by donor ligands to produce Cp$_2$Ta(L)(CH$_2$SiH(*t*-Bu)$_2$) (**4a,b**; L = CO, PMe$_3$). The reaction of **1** with H$_2$Si(*t*-Bu)$_2$ in benzene also produces the phenyl methylene complex Cp$_2$Ta(=CH$_2$)(Ph) (**5**) in addition to **2**, as a result of competing benzene C–H activation during the reaction. Finally, the order of relative rates for ligand to alkylidene migratory insertion in complexes of the type Cp$_2$Ta(=CHR)(X) is observed to be X = H > SiH(*t*-Bu)$_2$ ≫ Ph > Me. Compounds **3** and **4a** have been structurally characterized by single-crystal X-ray diffraction methods (**3**, triclinic, *P*$\bar{1}$, $Z$ = 2, $a$ = 8.001 (1) Å, $b$ = 10.389 (1) Å, $c$ = 13.747 (2) Å, α = 68.80 (1)°, β = 78.49 (1)°, γ = 76.97 (1)°, $V$ = 1029.1 Å$^3$; **4a**, monoclinic, $C2/c$, $Z$ = 8, $a$ = 30.922 (4) Å, $b$ = 8.094 (2) Å, $c$ = 20.517 (3) Å, β = 96.15 (1)°, $V$ = 5105.2 Å$^3$).

## Introduction

Many important reactions of transition-metal carbene and alkylidene complexes involve the net transfer of a carbene fragment to an unsaturated substrate. Common examples utilizing organic substrates include cyclopropanation of olefins,[2] olefin metathesis,[3] conversion of

(1) Alfred P. Sloan Fellow, 1990–1992.

(2) Reviews: (a) Doyle, M. P. In *Catalysis of Organic Reactions*; Augustine, R. L., Ed.; Marcel Dekker: New York, 1985. (b) Burke, S. D.; Grieco, P. A. *Org. React.* **1979**, *26*, 361.

0276-7333/90/2309-2952$02.50/0 

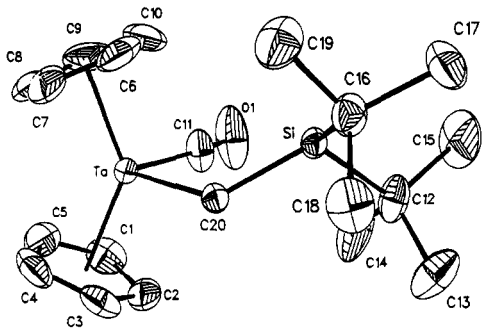


**Figure 1.** ORTEP drawing of $Cp_2Ta(CO)(CH_2SiH(t\text{-}Bu)_2)$, **4a**, showing 30% probability thermal ellipsoids.

carbonyl compounds to olefins,[4] and synthesis of fused-ring organic compounds from alkynes.[5] Unsaturated transition-metal centers have also been shown to react with metal carbene and alkylidene complexes, generally yielding binuclear species with the divalent carbon ligand bridging both metals.[6,7] The present contribution describes our investigations of the reactions of the alkylidene complex $Cp_2Ta(=CH_2)(CH_3)$ (**1**) with organohydrosilanes. These studies have led us to conclude that **1** reacts with silanes by mechanistic pathways which are strongly dependent upon the steric bulk of the silane and that for the bulky silane $H_2Si(t\text{-}Bu)_2$ the pathway involves a novel chain mechanism involving methylene transfer between tantalum centers. Furthermore, methylene transfer between $Cp_2Ta$ centers has been found to be a fairly common phenomenon. Finally, the intramolecular migratory insertion of silyl and phenyl groups to methylene ligands has been observed, allowing the qualitative ranking of migratory aptitudes for complexes of the formula $Cp_2Ta(X)(=CHR)$ (X = H, $SiH(t\text{-}Bu)_2$, Ph, Me).

## Results

**Reactions of $Cp_2Ta(=CH_2)(Me)$ with Silanes in THF.** $Cp_2Ta(=CH_2)(Me)$ (**1**) reacts with relatively unhindered silanes such as $Me_2SiH_2$ and $Me_3SiH$ in tetrahydrofuran (THF) to produce $Cp_2Ta(H_2C{=}CH_2)(Me)$ and the bis(silyl) complexes $Cp_2Ta(SiR_3)_2(H)$ ($SiR_3$ = $SiMe_2H$, $SiMe_3$) in approximately equal amounts with concurrent liberation of methane (eq 1). The reaction requires ca.

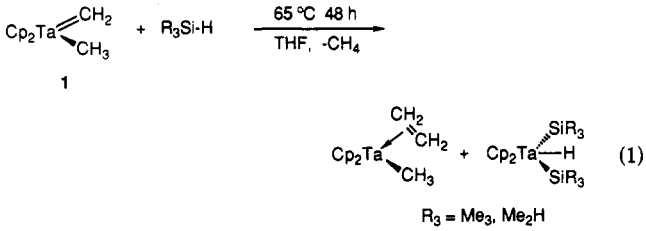

(1)

30 days at 25 °C or 2 days at 65 °C to reach completion. The bis(silyl) complexes have been previously prepared by the reaction of the silanes with $Cp_2Ta(Me)(L)$ (L = $PMe_3$, $C_2H_4$) under thermal (100 °C) or photochemical (350 nm) conditions.[8,9]

In contrast, reaction of **1** with $H_2Si(t\text{-}Bu)_2$ in THF does not proceed to the bis(silyl) complex. In this instance, the silyl-substituted alkylidene hydride complex $Cp_2Ta(H)(=CHSiH(t\text{-}Bu)_2)$ (**2**) is formed in good yield as determined by $^1H$ NMR spectroscopy after 3 days at 25 °C, or 1.5 h at 65 °C (eq 2). Only small amounts of $Cp_2Ta(H_2C{=}CH_2)(Me)$ are formed (<5%). Note that reaction of **1** with $H_2Si(t\text{-}Bu)_2$ proceeds substantially *faster* than with the less hindered silanes. In addition to **2**, varying amounts (<30%) of the bridging alkylidene complex $\{CpTa(\mu_2\text{-}\eta^1{:}\eta^5\text{-}C_5H_4)\}_2(\mu\text{-}C(H)(SiH(t\text{-}Bu)_2))$ (**3**) are also produced (vide infra).

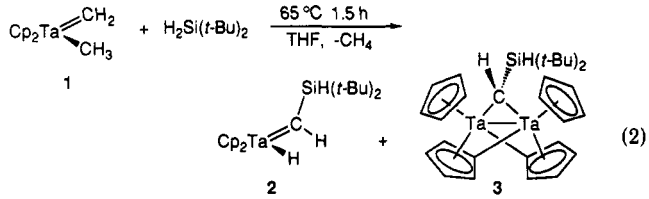

(2)

Compound **2** has been isolated as a green oily solid and has been characterized by NMR spectroscopy ($^1H$ and $^{13}C$) and chemical derivatization. The $^1H$ NMR spectrum of **2** exhibits a doublet at $\delta$ 10.50 for the alkylidene proton, which is coupled to the silicon hydride resonance at $\delta$ 4.03 ($^3J_{HH}$ = 7.3 Hz). The low field chemical shift of the alkylidene proton resonance is typical of those found in related systems.[10,11] The tantalum hydride gives rise to a singlet at $\delta$ 1.39, similar to the value of $\delta$ 1.75 observed for the tantalum methylidene hydride complex $Cp^*_2Ta(=CH_2)(H)$ ($Cp^* \equiv \eta^5\text{-}C_5Me_5$).[11] Two resonances are observed for the Cp ligands in **2** ($\delta$ 5.61, 5.56), resulting from the expected "perpendicular" orientation of the unsymmetrically substituted alkylidene. This orientation, in which the carbon p orbital is coplanar with the valence orbitals on the bent metallocene, maximizes Ta–C $\pi$ bonding. This asymmetry also results in diastereotopic *t*-Bu groups on silicon, observed at $\delta$ 0.93 and 0.85. The $^{13}C$ NMR spectrum of **2** exhibits a characteristic downfield shift for the alkylidene carbon at $\delta$ 234.8 ($^1J_{CH}$ = 126.7 Hz).

As the oily nature of **2** prevented isolation of analytically pure samples, a more tractable derivative was desired. Treatment of **2** with carbon monoxide yields the tantalum carbonyl alkyl complex $Cp_2Ta(CO)(CH_2SiH(t\text{-}Bu)_2)$ (**4a**; eq 3). The formation of **4a** occurs immediately at 25 °C

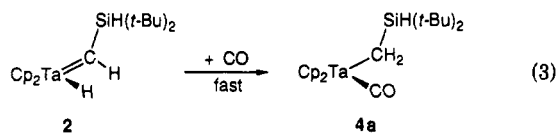

(3)

upon the introduction of CO to solutions of **2**. Analytically pure **4a** has been isolated in 62% yield (based on **1**) by a two-step synthesis in which **2** is initially prepared and then treated with CO. Compound **4a** exhibits an $^1H$ NMR spectrum (benzene-$d_6$) in which a single Cp resonance is observed, reflecting free rotation at the tantalum alkyl bond. In addition, the tantalum hydride and alkylidene proton resonances of **2** have been replaced with a doublet at $\delta$ −1.37 corresponding to the $CH_2$ group coupled to the silicon hydride, which is observed as a triplet at $\delta$ 3.81 ($^3J_{HH}$

(3) Reviews: (a) Grubbs, R. H. *Prog. Inorg. Chem.* **1978**, *24*, 1. (b) Mol, J. C. *J. Mol. Catal.* **1982**, *15*, 35.
(4) (a) Shrock, R. R. *J. Am. Chem. Soc.* **1976**, *98*, 5399. (b) Brown-Wensley, K. A.; Buchwald, S. L.; Cannizzo, L.; Clawson, L.; Ho, S.; Meinhardt, D.; Stille, J. R.; Straus, D., Grubbs, R. H. *Pure Appl. Chem.* **1983**, *55*, 1733.
(5) Reviews: (a) Dotz, K. H. *Angew. Chem., Int. Ed. Engl.* **1984**, *23*, 587. (b) Wulff, W. D.; Tang, P. C.; Chan, K. S., McCallum, J. S.; Yang, D. C.; Gilbertson, S. R. *Tetrahedron* **1985**, *41*, 5813.
(6) (a) Howard, J. A. K.; Mead, K. A.; Moss, J. R.; Navarro, R.; Stone, F. G. A. *J. Chem. Soc., Dalton Trans.* **1981**, 743. (b) Ashworth, T. V.; Howard, J. A. K.; Laguna, M.; Stone, F. G. A. *J. Chem. Soc., Dalton Trans.* **1980**, 1593. (c) Berry, M.; Howard, J. A. K.; Stone, F. G. A. *J. Chem. Soc., Dalton Trans.* **1980**, 1601.
(7) (a) Jacobsen, E. N.; Goldberg, K. I.; Bergman, R. G. *J. Am. Chem. Soc.* **1988**, *110*, 3706–3707. (b) Goldberg, K. I.; Bergman, R. G. *J. Am. Chem. Soc.* **1988**, *110*, 4853–4855.
(8) Berry, D. H.; Jiang, Q. *J. Am. Chem. Soc.* **1989**, *111*, 8049–8051.
(9) Jiang, Q.; Koloski, T. S.; Carroll, P. J.; Berry, D. H., manuscript in preparation.
(10) Schrock, R. R. *Acc. Chem. Res.* **1979**, *12*, 98.
(11) van Asselt, A.; Burger, B. J.; Gibson, V. C.; Bercaw, J. E. *J. Am. Chem. Soc.* **1986**, *108*, 5347.

**Table I. Summary of Structure Determinations**

| | 3 | 4a |
|---|---|---|
| formula | $C_{29}H_{38}SiTa_2$ | $C_{20}H_{31}OSiTa$ |
| fw | 776.61 | 496.50 |
| crystal class | monoclinic | triclinic |
| cryst dimens, mm | 0.33 × 0.25 × 0.21 | 0.37 × 0.28 × 0.22 |
| space group | $C2/c$ | $P\bar{1}$ |
| $Z$ | 8 | 2 |
| cell consts | | |
| $a$, Å | 30.922 (4) | 8.001 (1) |
| $b$, Å | 8.094 (2) | 10.389 (1) |
| $c$, Å | 20.517 (3) | 13.747 (2) |
| $\alpha$, deg | | 68.80 (1) |
| $\beta$, deg | 96.15 (1) | 78.49 (1) |
| $\gamma$, deg | | 76.97 (1) |
| $V$, Å$^3$ | 5105.2 | 1029.1 |
| $\mu$, cm$^{-1}$ | 85.31 | 53.38 |
| $D_{calc}$, g/cm$^3$ | 2.021 | 1.602 |
| $F(000)$ | 2976 | 492 |
| radiation | Mo $K_\alpha$ ($\lambda$ = 0.71073 Å) | Mo $K_\alpha$ |
| $\theta$ range, deg | 2–27.5 | 2–27.5 |
| scan mode | $\omega$–2$\theta$ | $\omega$–2$\theta$ |
| $hkl$ collected | ±40,–10,26 | ±10,±13,–17 |
| no. of rflns measd | 6441 | 4911 |
| no. of unique rflns measd | 5857 | 4712 |
| no. of rflns used in refinement | 4144 (>3$\sigma$) | 4067 (>3$\sigma$) |
| no. of params | 289 | 208 |
| data param ratio | 14.3 | 19.6 |
| $R_1$ | 0.030 | 0.023 |
| $R_2$ | 0.037 | 0.031 |
| GOF | 1.037 | 0.989 |

= 2.7 Hz). A single *t*-Bu resonance is also observed. The carbonyl ligand exhibits a resonance at $\delta$ 264 in the $^{13}C$ NMR and an absorption at 1894 cm$^{-1}$ in the infrared spectrum. The phosphine analogue $Cp_2Ta(PMe_3)(CH_2SiH(t\text{-}Bu)_2)$ (**4b**) is similarly produced by treatment of **2** with $PMe_3$. Compound **4b** was not isolated as a pure substance, as loss of $PMe_3$ under vacuum at 25 °C leads to regeneration of **2**.

The structure of **4a** as determined by single-crystal X-ray diffraction methods is shown in Figure 1. Crystallographic details are summarized in Table I. Bond distances and angles are listed in Tables II and III. The geometry at tantalum is typical for a bent metallocene complex; the two Cp ring centroids subtend an angle of 135.5°, and the carbonyl and alkyl ligands form an angle of 95.4 (2)° at the metal. The carbonyl ligand is relatively linear ($\angle$Ta–C11–O = 172.5 (5)°). The silyl-substituted alkyl ligand exhibits a slightly distorted tetrahedral geometry at the carbon atom ($\angle$Ta–C20–Si = 125.7 (2)°), and the Si–C20 distance of 1.852 (3) Å is somewhat shorter than typical Si–C distances (1.87–1.91 Å).[12]

Significantly, the simultaneous reaction of **1**, $H_2Si(t\text{-}Bu)_2$, and CO in a single reaction vessel does not yield **4a**. Under these conditions, *essentially no reaction with $H_2Si(t\text{-}Bu)_2$ is observed.* Small quantities of $Cp_2Ta(Me)(H_2C{=}CH_2)$ and $Cp_2Ta(Me)(CO)$ (1:1, <10% total conversion after days at 25 °C) are the only products detected (eq 4). These are the expected products of the

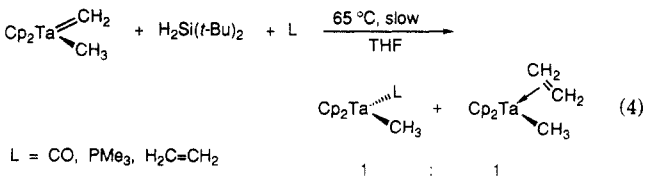


(4)

L = CO, $PMe_3$, $H_2C{=}CH_2$

(12) (a) Bazant, V.; Chvalovsky, V.; Rathousky, J. *Organosilicon Compounds*; Academic Press: New York, 1965; p 179. (b) Gordon, A. J.; Ford, R. A. *The Chemist's Companion*; Wiley: New York, 1972; p 107 and references therein.

**Table II. Selected Bond Distances in 4a**[a]

| atom 1 | atom 2 | dist, Å | atom 1 | atom 2 | dist, Å |
|---|---|---|---|---|---|
| Ta | C1 | 2.364 (5) | C1 | C5 | 1.349 (8) |
| Ta | C2 | 2.355 (4) | C2 | C3 | 1.379 (9) |
| Ta | C3 | 2.389 (5) | C3 | C4 | 1.334 (8) |
| Ta | C4 | 2.389 (5) | C4 | C5 | 1.40 (1) |
| Ta | C5 | 2.371 (5) | C6 | C7 | 1.381 (8) |
| Ta | C6 | 2.402 (5) | C6 | C10 | 1.36 (1) |
| Ta | C7 | 2.383 (5) | C7 | C8 | 1.41 (1) |
| Ta | C8 | 2.328 (6) | C8 | C9 | 1.39 (1) |
| Ta | C9 | 2.337 (6) | C9 | C10 | 1.410 (9) |
| Ta | C10 | 2.373 (5) | C11 | O1 | 1.148 (7) |
| Ta | C11 | 2.025 (5) | C12 | C13 | 1.52 (1) |
| Ta | C20 | 2.321 (4) | C12 | C14 | 1.500 (8) |
| Si | C12 | 1.928 (4) | C12 | C15 | 1.520 (8) |
| Si | C16 | 1.923 (5) | C16 | C17 | 1.533 (7) |
| Si | C20 | 1.852 (3) | C16 | C18 | 1.523 (9) |
| Si | HSi | 1.403 | C16 | C19 | 1.535 (7) |
| C1 | C2 | 1.406 (9) | | | |

[a] Numbers in parentheses are estimated standard deviations in the least significant digits.

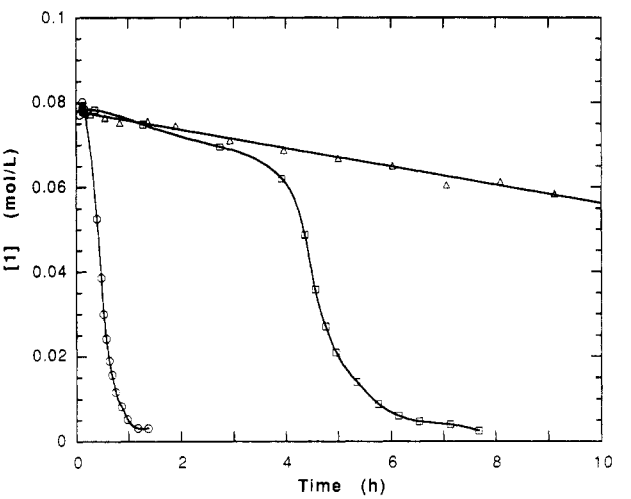


**Figure 2.** Plot of [1] vs time for reaction of **1** in THF at 51 °C with (a) $H_2Si(t\text{-}Bu)_2$ (○), (b) $H_2Si(t\text{-}Bu)_2$ and 0.1 equiv of $PMe_3$ (□), and (c) excess $PMe_3$ (no silane) (△). Solid lines are included for clarity only.

disproportionation of **1** in the presence of donor ligands as reported by Schrock and Sharp.[13] Other ligands such as $PMe_3$ and $H_2C{=}CH_2$ also inhibit the reaction of **1** with $H_2Si(t\text{-}Bu)_2$.

The dramatic effect of added $PMe_3$ on the reaction of **1** with $H_2Si(t\text{-}Bu)_2$ at 51 °C in THF is illustrated in Figure 2, in which the disappearance of **1** vs time (monitored by $^1H$ NMR spectroscopy) is plotted for the reaction run (a) in the absence of $PMe_3$ (○) and (b) with 0.1 equiv of added phosphine (□). In addition, the disappearance of **1** in the absence of silane but with 3 equiv of $PMe_3$ added is also shown (△). With no added $PMe_3$, disappearance of **1** occurs rapidly after a short induction period. Approximately 50% conversion is observed after 30 min under these conditions. In the presence of excess $PMe_3$ but without silane, however, only ca. 25% conversion is observed after >10 h. In this instance, only $Cp_2Ta(Me)(H_2C{=}CH_2)$ and $Cp_2Ta(Me)(PMe_3)$ are observed as products. In addition, a plot of $[1]^{-1}$ vs time for the reaction with phosphine is linear, consistent with the expected second-order dependence on [1] ($k = 1.32 \times 10^{-4}$ M$^{-1}$ s$^{-1}$). The reaction of **1** with $H_2Si(t\text{-}Bu)_2$ in the presence of 0.1 equiv of $PMe_3$ has features in common with both of the previous experiments. Disappearance of **1** initially proceeds considerably slower

(13) Schrock, R. R.; Sharp, P. R. *J. Am. Chem. Soc.* **1978**, *100*, 2389.

**Table III. Selected Bond Angles in 4a[a]**

| atom 1 | atom 2 | atom 3 | angle, deg | atom 1 | atom 2 | atom 3 | angle, deg |
|---|---|---|---|---|---|---|---|
| Cp1[b] | Ta | Cp2[b] | 135.0 | C8 | C9 | C10 | 106.8 (7) |
| C11 | Ta | C20 | 95.4 (2) | C6 | C10 | C9 | 108.2 (6) |
| C12 | Si | C16 | 113.0 (2) | Ta | C11 | O1 | 172.5 (5) |
| C12 | Si | C20 | 111.7 (2) | Si | C12 | C13 | 112.3 (4) |
| C12 | Si | HSi | 104.2 (2) | Si | C12 | C14 | 110.1 (4) |
| C16 | Si | C20 | 111.0 (2) | Si | C12 | C15 | 111.5 (4) |
| C16 | Si | HSi | 109.0 | C13 | C12 | C14 | 108.0 (5) |
| C20 | Si | HSi | 107.5 | C13 | C12 | C15 | 106.9 (5) |
| C2 | C1 | C5 | 107.2 (6) | C14 | C12 | C15 | 107.8 (6) |
| C1 | C2 | C3 | 107.6 (5) | Si | C16 | C17 | 113.0 (4) |
| C2 | C3 | C4 | 108.1 (6) | Si | C16 | C18 | 112.8 (3) |
| C3 | C4 | C5 | 109.0 (5) | Si | C16 | C19 | 107.2 (4) |
| C1 | C5 | C4 | 108.0 (5) | C17 | C16 | C18 | 109.5 (4) |
| C7 | C6 | C10 | 109.9 (6) | C17 | C16 | C19 | 107.3 (4) |
| C6 | C7 | C8 | 106.5 (6) | C18 | C16 | C19 | 106.7 (5) |
| C7 | C8 | C9 | 108.6 (5) | Ta | C20 | Si | 125.7 (2) |

[a] Numbers in parentheses are estimated standard deviations in the least significant digits. [b] Cp1 and Cp2 refer to the $C_5H_5$ ring centroids.

than in the absence of $PMe_3$, with 20% conversion requiring ca. 4 h. At this point, virtually all of the $PMe_3$ has been consumed, with concomitant formation of $Cp_2Ta(Me)(PMe_3)$ and $Cp_2Ta(Me)(H_2C{=}CH_2)$ (ca. 1:1). A small amount of **4b** is also detected. Following consumption of the phosphine, however, subsequent disappearance of **1** is rapid, reaching 90% completion after an additional 2 h. Compounds **2** and **3** are now formed as reaction products.

**Reactions of $Cp_2Ta(=CH_2)(Me)$ with Silanes in Benzene.** The reaction of $Me_3SiH$ with **1** proceeds in benzene to yield the bis(silyl) complex and $Cp_2Ta(H_2C{=}CH_2)(Me)$ (ca. 1:1), as was also observed in THF. Plots of $[1]^{-1}$ vs time from kinetics measurements of this reaction (benzene-$d_6$, 67 °C, $[1]_0$ = 0.09–0.18 M) are linear through >87% conversion, consistent with second-order dependence on [1] ($k$ = (1.04–1.15) × $10^{-3}$ $M^{-1}$ $s^{-1}$). No dependence of the rate on $[Me_3SiH]$ in the range 0.9–1.8 M was observed. The rate for the disproportionation of **1** with $PMe_3$ in the absence of silane at 67 °C also exhibits a second-order dependence on [1] with $k$ = 8.5 × $10^{-4}$ $M^{-1}$ $s^{-1}$.[14]

In contrast, the reaction of **1** with $H_2Si(t\text{-}Bu)_2$ in benzene exhibits two notable differences compared with the reaction in THF; the reaction is considerably faster in benzene (completion reached within 6 h at 25 °C) and the tantalum *phenyl* methylene complex $Cp_2Ta(=CH_2)(Ph)$ (**5**) is produced in addition to **2** and **3** (ca. 3:2:1) (eq 5). As the

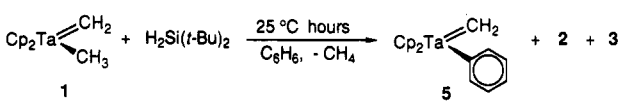


(5)

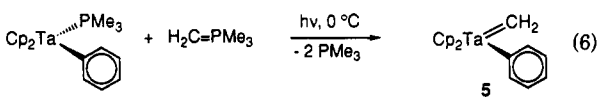


(6)

separation of this reaction mixture was not feasible, **5** was prepared in 37% yield by photolysis of $Cp_2Ta(Ph)(PMe_3)$ in the presence of methylenetrimethylphosphorane at 0 °C (eq 6). The $^1H$ NMR spectrum (benzene-$d_6$) of **5** exhibits single methylene and Cp resonances at $\delta$ 10.64 (2 H) and 5.10 (10 H) in addition to multiplets due to the phenyl protons. The methylene carbon exhibits a resonance at $\delta$ 239.1 ($^1J_{CH}$ = 132 Hz) in the $^{13}C$ NMR spectrum.

**Ligand to Alkylidene Migrations.** Three new alkylidene complexes prepared in this study undergo reactions in which a ligand is transferred from tantalum to the alkylidene carbon. In the first instance, formation of **4a** and **4b** from **2**, a hydride has migrated from tantalum to the alkylidene to yield a silyl-substituted alkyl ligand (eq 3).

Migration of a phenyl group in the phenyl methylene complex **5** is also observed. Although **5** is relatively stable in solution at 25 °C, clean conversion to the benzyl complex $Cp_2Ta(PMe_3)(CH_2Ph)$ (**6**) is complete within 5 h at 65 °C in benzene in the presence of phosphine (eq 7). Com-

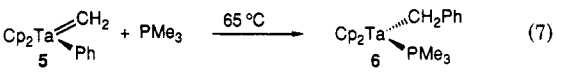


(7)

pound **6** results from the migration of phenyl to the methylidene ligand, and association of phosphine. The benzyl complex was not isolated, and the structure was assigned on the basis of the $^1H$ and $^{13}C$ NMR spectra. The $^1H$ NMR spectrum exhibits resonances at $\delta$ 4.21 (d, Cp, $J_{P\text{-}H}$ = 1.8 Hz), 1.67 (d, $CH_2Ph$, $J_{P\text{-}H}$ = 4.8 Hz), and 0.81 (d, $P(CH_3)_3$, $J_{P\text{-}H}$ = 7.0 Hz), as well as resonances for the phenyl protons. In the absence of added donor ligands, **5** decomposes at 65 °C to a complex mixture of products.

Silyl group migration from tantalum to an alkylidene is facile even at −10 °C. The silyl methylene complex $Cp_2Ta(=CH_2)(SiH(t\text{-}Bu)_2)$ (**7**) can be generated in solution by photolysis (350 nm) of $Cp_2Ta(PMe_3)(SiH(t\text{-}Bu)_2)$ in the presence of $Me_3P{=}CH_2$ at −70 °C (eq 8). The $^1H$ NMR

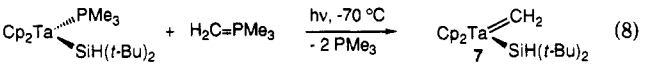


(8)

spectrum of **7** at −70 °C indicates that rotation of the bulky silyl group is slow on the NMR time scale, giving rise to chemically inequivalent pairs of Cp ($\delta$ 5.61, 5.43) and $t$-Bu ($\delta$ 1.34, 1.32) ligands. The methylene protons are also inequivalent and exhibit an AB quartet centered at $\delta$ 10.44. Coalescence of the Cp resonances of **7** is observed at ca. −20 °C, corresponding to a $\Delta G^{\ddagger}$ of 17.1 kcal·mol$^{-1}$ for rotation around the tantalum–silyl bond.

Compound **7** reacts within minutes at −10 °C to form **4b**, the phosphine-trapped alkyl complex, which results from silyl group migration from tantalum to the methylene ligand and association of phosphine (eq 9). Phosphine is unavoidably present as a result of the synthesis of **7** in situ.

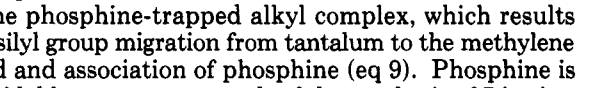


(9)

**Alkylidene-Transfer Reactions between Tantalum Centers.** Several reactions were examined in which net

(14) A value of $k$ = 5.4 × $10^{-4}$ $M^{-1}$ $s^{-1}$ was measured at 60 °C in benzene-$d_6$ by Schrock and Sharp.[13]

transfer of a methylidene group between tantalum centers was observed. This process is exemplified by the crossover reaction between $Cp_2Ta(=CH_2)(Me)$ and $CpCp'Ta(Me)(PMe_3)$ ($Cp' = CH_3C_5H_4$). As shown in eq 10, these

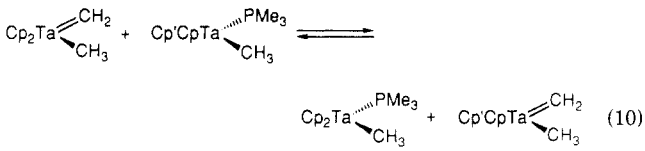

(10)

complexes react slowly at room temperature in benzene to produce an equilibrium mixture containing $Cp_2Ta(Me)(PMe_3)$ and $CpCp'Ta(=CH_2)(Me)$, in addition to the starting complexes. Trace amounts of $Cp_2Ta(Me)(H_2C=CH_2)$ and $CpCp'Ta(Me)(H_2C=CH_2)$ are also formed. The equilibrium in eq 10 has also been established from an initial mixture of $Cp_2Ta(Me)(PMe_3)$ and $CpCp'Ta(=CH_2)(Me)$.

Intermolecular methylene transfer is also indicated in the synthesis of **2** and **5** by using **1** as the methylene source. For example, treatment of the phosphine phenyl complex $Cp_2Ta(Ph)(PMe_3)$ with **1** in benzene at 50 °C yields **5** and $Cp_2Ta(Me)(PMe_3)$ (eq 11). Similarly, the phosphine silyl

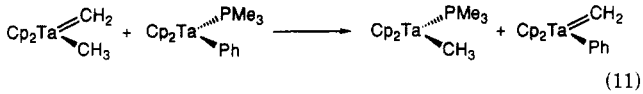

(11)

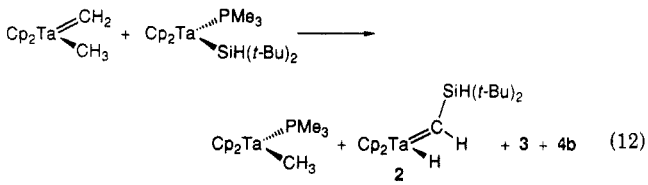

(12)

complex $Cp_2Ta(SiH(t\text{-}Bu)_2)(PMe_3)$ reacts with **1** in THF at 25 °C to yield a mixture of **2**, **3**, **4b**, and $Cp_2Ta(Me)(PMe_3)$ (1:3.3:1.8:6.5) (eq 12). Note that compounds **2**, **3**, and **4b** can all be derived from the unstable methylene silyl complex **7** (vide supra).

**Synthesis and Structure of $\{CpTa(\mu_2\text{-}\eta^1\text{:}\eta^5\text{-}C_5H_4)\}_2(\mu\text{-}C(H)(SiH(t\text{-}Bu)_2))$, 3.** As described above, the bridging alkylidene **3** is a minor product that accompanies the formation of **2** from **1** and $H_2Si(t\text{-}Bu)_2$. Analytically pure **3** has been isolated in good yield from the reaction of the Ta(III) silyl complex $Cp_2Ta(PMe_3)(SiH(t\text{-}Bu)_2)$ with excess $Cp_2Ta(=CH_2)(CH_3)$ at 65 °C in THF as shown in eq 13 (86% based on silyl complex). Large amounts of

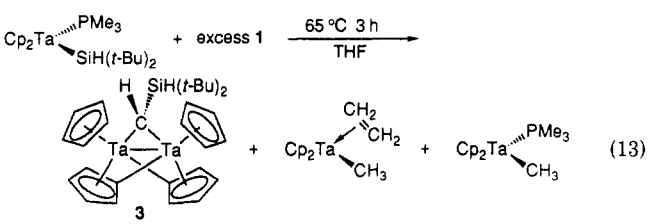

(13)

$Cp_2Ta(PMe_3)(Me)$ and $Cp_2Ta(H_2C=CH_2)(Me)$ are also formed as byproducts under these conditions and can be removed by sublimation. The $^1H$ NMR spectrum of **3** exhibits two singlets for the Cp rings and two sets of resonances for the $C_5H_4$ ligands. The inequivalence of the rings is a result of their trans disposition and the unsymmetric substitution at the alkylidene bridge. The alkylidene proton gives rise to a doublet at $\delta$ 2.62, coupled to the silicon hydride ($\delta$ 4.67, $^3J_{HH}$ = 2.9 Hz). The $^{13}C$ NMR spectrum of **3** is consistent with the proton spectrum, and all assignments have been confirmed by two-dimensional heteronuclear COSY NMR spectroscopy.

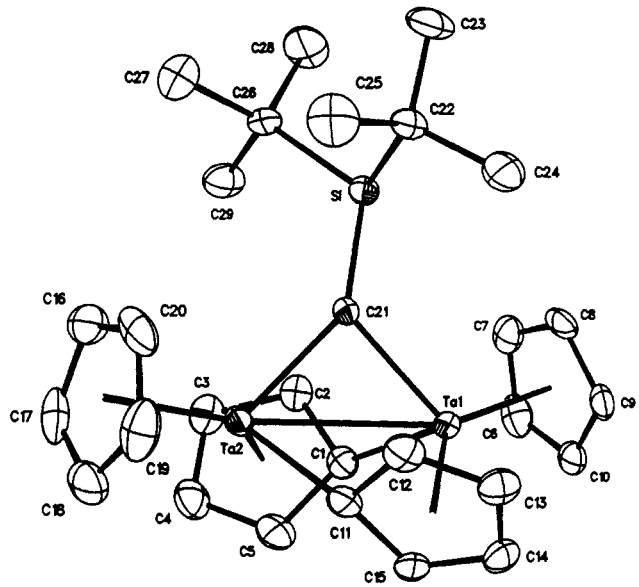


**Figure 3.** ORTEP drawing of $\{CpTa(\mu_2\text{-}\eta^1\text{:}\eta^5\text{-}C_5H_4)\}_2(\mu\text{-}C(H)(SiH(t\text{-}Bu)_2))$, **3**, showing 30% probability thermal ellipsoids.

**Table IV. Selected Bond Distances in 3**[a]

| atom 1 | atom 2 | dist, Å | atom 1 | atom 2 | dist, Å |
|---|---|---|---|---|---|
| Ta1 | Ta2 | 2.9642 (4) | C12 | C13 | 1.52 (1) |
| Ta1 | C1 | 2.195 (7) | C12 | C14 | 1.500 (8) |
| Ta1 | C6 | 2.456 (8) | C12 | C15 | 1.520 (8) |
| Ta1 | C7 | 2.463 (9) | C16 | C17 | 1.533 (7) |
| Ta1 | C8 | 2.446 (7) | C16 | C18 | 1.523 (9) |
| Ta1 | C9 | 2.418 (7) | C16 | C19 | 1.535 (7) |
| Ta1 | C10 | 2.414 (8) | Si | C21 | 1.863 (7) |
| Ta1 | C11 | 2.213 (7) | Si | C22 | 1.937 (8) |
| Ta1 | C12 | 2.367 (8) | Si | C26 | 1.942 (7) |
| Ta1 | C13 | 2.478 (8) | Si | HSi | 1.414 |
| Ta1 | C14 | 2.430 (8) | C1 | C2 | 1.45 (1) |
| Ta1 | C15 | 2.280 (8) | C1 | C5 | 1.45 (1) |
| Ta1 | C21 | 2.264 (6) | C2 | C3 | 1.40 (1) |
| Ta2 | C1 | 2.215 (7) | C3 | C4 | 1.40 (1) |
| Ta2 | C2 | 2.371 (7) | C4 | C5 | 1.42 (1) |
| Ta2 | C3 | 2.475 (8) | C6 | C7 | 1.40 (1) |
| Ta2 | C4 | 2.417 (9) | C6 | C10 | 1.39 (1) |
| Ta2 | C5 | 2.287 (8) | C7 | C8 | 1.41 (1) |
| Ta2 | C11 | 2.201 (7) | C8 | C9 | 1.41 (1) |
| Ta2 | C16 | 2.441 (8) | C9 | C10 | 1.40 (1) |
| Ta2 | C17 | 2.413 (8) | C11 | C12 | 1.47 (1) |
| Ta2 | C18 | 2.409 (9) | C11 | C15 | 1.46 (1) |
| Ta2 | C19 | 2.461 (9) | C12 | C13 | 1.40 (1) |
| Ta2 | C20 | 2.487 (9) | C13 | C14 | 1.42 (1) |
| Ta2 | C21 | 2.248 (6) | C14 | C15 | 1.39 (1) |
| C1 | C2 | 1.406 (9) | C16 | C17 | 1.40 (1) |
| C1 | C5 | 1.349 (8) | C16 | C20 | 1.38 (1) |
| C2 | C3 | 1.379 (9) | C17 | C18 | 1.38 (1) |
| C3 | C4 | 1.334 (8) | C18 | C19 | 1.40 (1) |
| C4 | C5 | 1.40 (1) | C19 | C20 | 1.39 (1) |
| C6 | C7 | 1.381 (8) | C22 | C23 | 1.54 (1) |
| C6 | C10 | 1.36 (1) | C22 | C24 | 1.52 (1) |
| C7 | C8 | 1.41 (1) | C22 | C25 | 1.52 (1) |
| C8 | C9 | 1.39 (1) | C26 | C27 | 1.55 (1) |
| C9 | C10 | 1.410 (9) | C26 | C28 | 1.52 (1) |
| C11 | O1 | 1.148 (7) | C26 | C29 | 1.53 (1) |

[a] Numbers in parentheses are estimated standard deviations in the least significant digits.

The solid-state structure of **3** was determined by a single-crystal X-ray diffraction study. An ORTEP representation of **3** is shown in Figure 3, and selected bond distances and angles in Tables IV and V. The dimer consists of two tantalocene fragments connected by two bridging $C_5H_4$ ligands and a silyl-substituted alkylidene bridge. All four $C_5$ rings are essentially planar. The displacement of the bridging carbons (C1 and C11) from the plane of their

**Table V. Selected Bond Angles in 3[a]**

| atom 1 | atom 2 | atom 3 | angle, deg | atom 1 | atom 2 | atom 3 | angle, deg |
|---|---|---|---|---|---|---|---|
| Cp2[b] | Ta1 | Cp3[b] | 134.4 | C6 | C10 | C9 | 107.9 (7) |
| Ta2 | Ta1 | Cp2[b] | 143.1 | Ta1 | C11 | Ta2 | 84.4 (3) |
| Ta2 | Ta1 | Cp3[b] | 81.8 | C12 | C11 | C15 | 102.4 (6) |
| Ta2 | Ta1 | C1 | 48.1 (2) | C11 | C12 | C13 | 109.7 (7) |
| Ta2 | Ta1 | C21 | 48.7 (2) | C12 | C13 | C14 | 108.9 (7) |
| C11 | Ta1 | C21 | 80.6 (3) | C13 | C14 | C15 | 107.3 (7) |
| Cp1[b] | Ta2 | Cp4[b] | 134.8 | C11 | C15 | C14 | 111.5 (7) |
| Ta1 | Ta2 | Cp1[b] | 80.8 | C17 | C16 | C20 | 106.0 (8) |
| Ta1 | Ta2 | Cp3[b] | 144.3 | C16 | C17 | C18 | 110.3 (8) |
| Ta1 | Ta2 | C11 | 48.0 (2) | C17 | C18 | C19 | 106.5 (8) |
| Ta1 | Ta2 | C21 | 49.2 (2) | C18 | C19 | C20 | 107.9 (8) |
| C1 | Ta2 | C21 | 83.1 (3) | C16 | C20 | C19 | 109.2 (8) |
| C21 | Si | C22 | 108.4 (3) | Ta1 | C21 | Ta2 | 82.1 (2) |
| C21 | Si | C26 | 119.4 (3) | Ta1 | C21 | Si | 127.6 (3) |
| C21 | Si | HSi | 112.3 | Ta2 | C21 | Si | 141.3 (3) |
| C22 | Si | C26 | 111.3 (3) | Si | C22 | C23 | 111.4 (5) |
| C22 | Si | HSi | 105.5 | Si | C22 | C24 | 110.0 (6) |
| C26 | Si | HSi | 98.8 | Si | C22 | C25 | 112.7 (5) |
| Ta1 | C1 | Ta2 | 84.5 (3) | C23 | C22 | C24 | 107.0 (6) |
| C2 | C1 | C5 | 105.0 (6) | C23 | C22 | C25 | 108.6 (7) |
| C1 | C2 | C3 | 109.3 (7) | C24 | C22 | C25 | 107.0 (7) |
| C2 | C3 | C4 | 108.5 (7) | Si | C26 | C27 | 114.7 (6) |
| C3 | C4 | C5 | 109.0 (7) | Si | C26 | C28 | 109.8 (5) |
| C1 | C5 | C4 | 108.1 (7) | Si | C26 | C29 | 109.8 (5) |
| C7 | C6 | C10 | 108.9 (7) | C27 | C26 | C28 | 107.5 (7) |
| C6 | C7 | C8 | 107.5 (7) | C27 | C26 | C29 | 108.0 (7) |
| C7 | C8 | C9 | 107.7 (7) | C28 | C26 | C29 | 106.8 (7) |
| C8 | C9 | C10 | 107.9 (7) | | | | |

[a] Numbers in parentheses are estimated standard deviations in the least significant digits. [b] Cp1, Cp2, Cp3, and Cp4 refer to the $C_5H_5$ ring centroids.

respective rings corresponds to a dihedral angle of only ca. 4°. The Ta1–C1 and Ta2–C11 bond vectors, however, lie an average of 32.8° below the $C_5H_4$ planes. The bridging alkylidene ligand is bound essentially symmetrically to the two metal centers, $D$(Ta–C21) = 2.264 (6) and 2.248 (6) Å.

Each tantalum is bonded to four anionic ligands, leading to a formal oxidation state of 4+ at each metal and $d^1$ electronic configurations. The Ta–Ta separation is 2.9642 (4) Å, within the expected range for a single bond, and is consistent with the observed diamagnetism of **3**. This Ta–Ta bond distance is substantially shorter than the Nb–Nb separation found in the related hydride dimer $\{CpNbH(\mu\text{-}\eta^5\text{:}\eta^1\text{-}C_5H_4)\}_2$ (3.105 (3) Å),[15] probably as a result of the small "bite angle" of the alkylidene bridge in **3**. Neglecting the Ta–Ta bond for the moment, it would appear that each tantalum center in **3** exhibits a normal metallocene coordination geometry, with the two bridging carbon ligands lying in the plane of the valence molecular orbitals (perpendicular to the plane of the two Ta–Cp ring centroid vectors). The metal–metal bond would then be formed by overlap of the remaining valence orbital on each tantalum. However, the three bridging ligands twist the two tantalocene fragments such that these orbitals are not directed toward one another; i.e., the Ta–Ta interaction can be described as a "bent bond".

Solutions of **3** in hydrocarbon solvents are intensely blue ($\lambda_{max}$ = 650 nm, $\epsilon$ = 2200). In contrast, the metallocene hydride dimers $\{CpM(H)(\mu\text{-}\eta^5\text{:}\eta^1\text{-}C_5H_4)\}_2$ (M = Nb, Ta) are yellow, even though these compounds have the same formal $d^1$–$d^1$ configurations and exhibit bent M–M bonds as found in **3**. The metal–metal bond in the hydride dimers, however, is formed by overlap of orbitals pointing to the outside of the metallocene wedges, whereas the closest Ta–Ta contact in **3** lies symmetrically between the bridging ligands at each metal. It is possible that the Ta–Ta orbital overlap in **3** is extremely poor and that a d–d or charge-transfer transition into the Ta–Ta $\sigma^*$ orbital occurs at correspondingly low energy. Alternatively, the low-energy electronic transition in **3** may be a new band resulting from the bridging alkylidene ligand.

## Discussion

There are several aspects of the reactions of silanes with $Cp_2Ta(=CH_2)(Me)$ that prompted more detailed studies. To begin with, the manner in which silanes initially interact with **1**, an 18e⁻, coordinatively saturated complex, is not immediately clear. Nucleophilic attack of the methylidene carbon at silicon would be one possibility, in analogy to the reaction of **1** with $Me_3SiBr$ reported by Schrock and Sharp.[13] Alternatively, direct addition of the Si–H bond across the Ta=C bond, in analogy to recent studies of zirconium imido complexes,[16] could also ultimately lead to the observed products. However, the results discussed below suggest that neither of these mechanisms are operative.

A second interesting aspect of the reaction of **1** with silanes is the surprising observation that the bulkier silane ($H_2Si(t\text{-}Bu)_2$) reacts considerably faster than less hindered silanes. In addition, the complete inhibition by donor ligands of the reaction of **1** with $H_2Si(t\text{-}Bu)_2$ is also unexpected, as the ligands would not appear able to interact with either **1** or the silane prior to formation of the product **2**.

**Mechanism of the Reaction of $Cp_2Ta(=CH_2)(Me)$ with $Me_3SiH$ and $Me_2SiH_2$.** The reactions of relatively small silanes with **1** would appear to be relatively straightforward. The fact that formation of the bis(silyl) complexes is accompanied by equal amounts of $Cp_2Ta(H_2C{=}CH_2)(Me)$ (eq 1) suggests the initial step of the reaction is the disproportionation of **1** described previ-

(15) (a) Guggenberger, L. J. *Inorg. Chem.* **1973**, *12*, 294. (b) Guggenberger, L. J.; Tebbe, F. N. *J. Am. Chem. Soc.* **1971**, *93*, 5924.

(16) (a) Walsh, P. J.; Hollander, F. J.; Bergman, R. G. *J. Am. Chem. Soc.* **1988**, *110*, 8729. (b) Cummings, C. C.; Baxter, S. M.; Wolczanski, P. T. *J. Am. Chem. Soc.* **1988**, *110*, 8731.

**Scheme I**

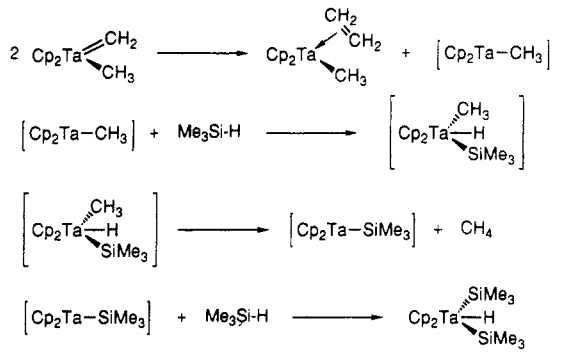

ously.[13] Consistent with this premise, the rate for reaction of $Me_3SiH$ with **1** (a) exhibits a second-order dependence on the concentration of **1**, (b) is independent of silane concentration, and (c) is virtually the same as that for disproportionation of **1** without silane in the presence of $PMe_3$. The disproportionation of **1** has previously been shown to proceed by bimolecular rate-limiting formation of $Cp_2Ta(H_2C{=}CH_2)(Me)$ and $Cp_2Ta(Me)$, a highly reactive 16e⁻ intermediate.[13] We have shown that this latter species, generated thermally or photochemically from $Cp_2Ta(L)(Me)$, reacts sequentially with unhindered silanes to produce $Cp_2Ta(H)(SiR_3)_2$ as shown in eq 14.[8,9] A mechanism for the reaction of **1** with small silanes based on the initial disproportionation of **1** is shown in Scheme I.

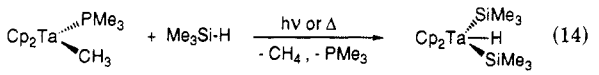

**Mechanism of the Reaction of $Cp_2Ta(=CH_2)(Me)$ with $H_2Si(t\text{-}Bu)_2$.** The reaction of **1** with $H_2Si(t\text{-}Bu)_2$ is substantially different than with the smaller silanes described above. Several points are noteworthy: (1) Only trace amounts of $Cp_2Ta(H_2C{=}CH_2)(Me)$ are produced along with **2**, and $Cp_2Ta(H_2C{=}CH_2)(Me)$ can be shown to be stable under the reaction conditions. (2) Reaction of **1** with $H_2Si(t\text{-}Bu)_2$ is much faster than the disproportionation of **1** in the presence of $Me_3SiH$ or ligands such as $PMe_3$. (3) The reaction of **1** with $H_2Si(t\text{-}Bu)_2$ is almost completely inhibited by even small amounts of added donor ligands (Figure 2), despite the fact that these ligands are not present in the reactants and therefore are not involved in dissociative preequilibria along the reaction coordinate leading to **2**.

The rapid reaction rate and absence of equimolar quantities of $Cp_2Ta(H_2C{=}CH_2)(Me)$ indicate that *stoichiometric* disproportionation of **1** is not necessary for reaction of **1** with $H_2Si(t\text{-}Bu)_2$. However, it would appear that $Cp_2Ta(Me)$, one of the two disproportionation products, is critical for the formation of **2**, because $Cp_2Ta(PMe_3)(Me)$ is the only product observed in addition to $Cp_2Ta(H_2C{=}CH_2)(Me)$ in the inhibited reaction of **1** with $H_2Si(t\text{-}Bu)_2$ in the presence of $PMe_3$. This ambiguity can be resolved if $Cp_2Ta(Me)$ plays a *catalytic* role in the formation of **2**. A possible reaction sequence involving the catalytic participation of $Cp_2Ta(Me)$ is shown in Scheme II.

In this sequence, the reaction is initiated by the disproportionation of **1** to form $Cp_2Ta(H_2C{=}CH_2)(Me)$ and $Cp_2Ta(Me)$. In the absence of donor ligands, $Cp_2Ta(Me)$ reacts with silane to ultimately produce $CH_4$ and the 16e⁻ silyl intermediate $Cp_2Ta(SiH(t\text{-}Bu)_2)$. This species reacts with **1** via a binuclear alkylidene transfer to yield $Cp_2Ta(=CH_2)(SiH(t\text{-}Bu)_2)$ with concurrent regeneration of $Cp_2Ta(Me)$. Migration of the silyl group to the alkyl-

**Scheme II**

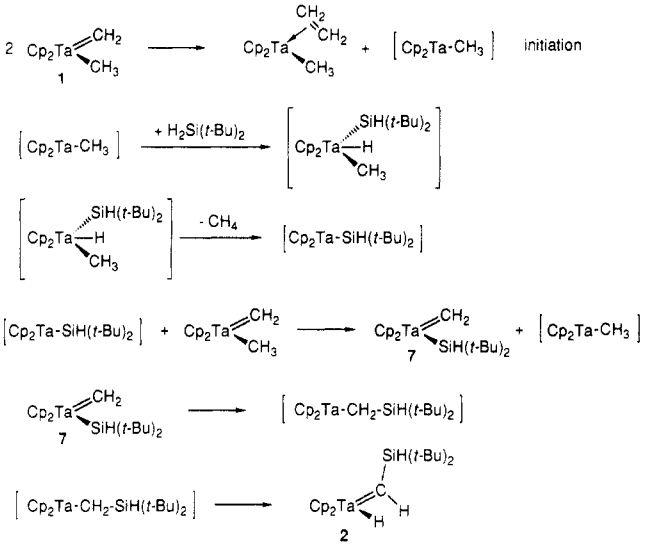

idene in $Cp_2Ta(=CH_2)(SiH(t\text{-}Bu)_2)$ generates the intermediate alkyl $Cp_2Ta(CH_2SiH(t\text{-}Bu)_2)$, which subsequently undergoes an $\alpha$-hydrogen elimination yielding **2**, the final product. The key feature of this mechanism, the catalytic participation of $Cp_2Ta(Me)$, bears a resemblance to free-radical chain reactions in which reactive odd-electron species generated during initiation are regenerated during product-forming steps.[17] In this instance, however, the chain-propagating species would be the 16e⁻ intermediate $Cp_2Ta(Me)$.

When the formation of **2** is attempted in the presence of donor ligands, $Cp_2Ta(Me)$ is rapidly trapped as $Cp_2Ta(L)(Me)$, blocking formation of the silyl and thus preventing reaction with additional **1** and regeneration of $Cp_2Ta(Me)$. Thus, the net reaction corresponds to the simple disproportionation of **1**. Note that reaction of $Cp_2Ta(L)(Me)$ with silanes is extremely slow at temperatures below ca. 100 °C.[8,9] Although quantitative analysis of the system was not attempted, this mechanism is consistent with the general features of the kinetics runs shown in Figure 2. Furthermore, it is possible to independently demonstrate the feasibility of each step of the proposed mechanism.

The initiation step which forms $Cp_2Ta(Me)$ is the disproportionation of **1** examined by Schrock and Sharp.[13] The net result of the second and third steps, formation of $Cp_2Ta(SiH(t\text{-}Bu)_2)$ from $Cp_2Ta(Me)$ and the silane has been previously observed in the synthesis of $Cp_2Ta(SiH(t\text{-}Bu)_2)(L)$ from $Cp_2Ta(Me)(L)$ under thermal (100 °C) or photochemical (350 nm) conditions.[8] The loss of methane most likely results from consecutive silane oxidative addition/methane reductive elimination steps as opposed to a concerted four-centered "$\sigma$-bond metathesis" process because (a) $\sigma$-bond metathesis has only been observed at highly electrophilic $d^0$ metal centers[18] whereas $Cp_2Ta(Me)$ is a Ta(III) ($d^2$) complex, and (b) Ta(V) bis(silyl) complexes $Cp_2Ta(H)(SiR_3)_2$, analogous to the proposed Ta(V) oxidative addition intermediate $Cp_2Ta(H)(Me)(SiH(t\text{-}Bu)_2)$, are extremely stable and most reason-

(17) See, for example: (a) *Free Radicals*; Kochi, J., Ed.; Wiley: New York, 1973; Vol. 2. (b) Halpern, J. *Pure Appl. Chem.* **1979**, *51*, 2171. (c) Byers, B. H.; Brown, T. L. *J. Am. Chem. Soc.* **1977**, *99*, 2527. (d) Berry, D. H.; Mitstifer, J. H. *J. Am. Chem. Soc.* **1987**, *109*, 3777.

(18) See, for example: (a) Watson, P. L.; Parshall, G. W. *Acc. Chem. Res.* **1985**, *18*, 51–56. (b) Fendrick, C. M.; Marks, T. J. *J. Am. Chem. Soc.* **1986**, *108*, 425–437. (c) Thompson, M. E.; Baxter, S. M.; Bulls, A. R.; Burger, B. J.; Nolan, M. C.; Santarsiero, B. D.; Schaefer, W. P.; Bercaw, J. E. *J. Am. Chem. Soc.* **1987**, *109*, 204–219. (d) Woo, H.-G.; Tilley, T. D. *J. Am. Chem. Soc.* **1989**, *111*, 8043.

ably arise from Si–H oxidation addition to an unsaturated Ta(III) silyl (cf. Scheme I and eq 1).

The fourth step in Scheme II requires the transfer of a methylene group from 1 to the unsaturated silyl, producing the silyl methylene intermediate $Cp_2Ta(=CH_2)(SiH(t\text{-}Bu)_2)$ (7) and regenerating $Cp_2Ta(Me)$. Analogous methylene-transfer reactions are found in the exchange between 1 and $CpCp'Ta(Me)(PMe_3)$ (eq 10) and in the formation of 5 from 1 and $Cp_2Ta(Ph)(PMe_3)$ (eq 11), reactions that most likely proceed via a binuclear intermediate containing a methylene bridge (eq 15).

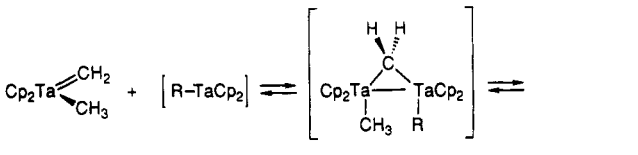

(15)

Bergman and co-workers have recently reported the characterization of several analogous heteronuclear complexes formed from 1, including $\{Cp_2Ta(Me)\}(\mu\text{-}CH_2)\{Pt(PMe_3)_2\}$ and $\{Cp_2Ta(Me)\}(\mu\text{-}CH_2)\{CpCo(PMe_3)\}$.[7] Com-

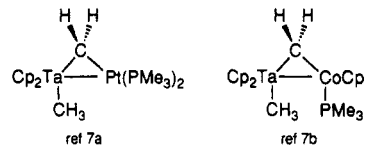

ref 7a ref 7b

pound 3 is another example of a binuclear tantalum alkylidene, although the bridging $C_5H_4$ ligands lend this compound greater stability than the proposed intermediate in eq 15. More generally, Stone and co-workers have reported the synthesis of a variety of binuclear alkylidene complexes by the reaction of unsaturated metal centers with mononuclear alkylidene or carbene complexes.[6]

Evidence for methylene transfer from 1 to $Cp_2Ta(SiH(t\text{-}Bu)_2)$ as proposed in Scheme II can also be inferred from the reaction of isolated $Cp_2Ta(SiH(t\text{-}Bu)_2)(PMe_3)$ with 1 to yield 2 and products derived from 2 (eq 12). Although the silyl methylene intermediate $Cp_2Ta(=CH_2)(SiH(t\text{-}Bu)_2)$ (7) is not directly observed in this reaction or in the reaction of 1 with $H_2Si(t\text{-}Bu)_2$, it can be produced and characterized at low temperatures by the photolysis of $Cp_2Ta(PMe_3)(SiH(t\text{-}Bu)_2)$ in the presence of $Me_3P{=}CH_2$ (eq 8). Compound 7 appears to be the first complex containing both silyl and alkylidene ligands. This method of generating 7 also produces 2 equiv of $PMe_3$ as a byproduct.

The fifth step in the proposed mechanism, migration of silyl from the metal to the methylene carbon, is suggested by the rapid conversion at ca. −10 °C of 7 to **4b**, the phosphine-trapped product of silyl migration (eq 9). Similar ligand migrations in closely related complexes are well precedented. The rapid silyl migration is not unexpected in light of the propensity for silyl group migration in other organometallic systems. There are precedents for silyl migration to the vast majority of ligands for which analogous migrations of hydride or alkyls are known,[19] including olefin,[20] carbonyl,[21] isocyanide,[22] and cyclopentadienyl[23] ligands.

In the case of the reaction of 1 with $H_2Si(t\text{-}Bu)_2$, the unsaturated alkyl $Cp_2Ta(CH_2SiH(t\text{-}Bu)_2)$ is generated in the absence of trapping ligands and $\alpha$-hydrogen elimination occurs to produce 2. Formation of alkylidene complexes by $\alpha$-hydrogen elimination is particularly well documented for tantalocene complexes[11,24] and is also indicated in the reversion of **4b** back to 2 upon removal of phosphine under vacuum (vide supra).

Finally, the formation of 3 by reaction of 2 with the intermediate $Cp_2Ta(Me)$ appears to act as the termination step in the chain reaction by consuming the key catalytic species (eq 16). Note that 3 is formed in high yield from

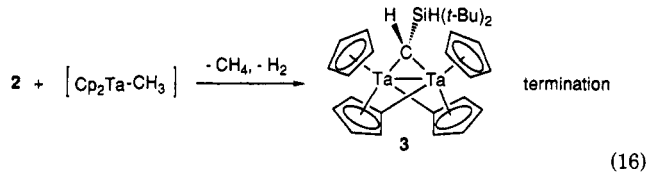

(16)

$Cp_2Ta(PMe_3)(SiH(t\text{-}Bu)_2)$ and excess 1 at 65 °C, conditions under which 2 will be generated in the presence of relatively high concentrations of $Cp_2Ta(Me)$.

Thus, supporting evidence can be provided for all of the proposed steps in Scheme II, and the catalytic or chain-carrying role of $Cp_2Ta(Me)$ accounts for the inhibition of the reaction by trace quantities of donor ligands. It is now also clear why $Me_3SiH$ reacts with 1 at a rate many times slower than the bulkier *tert*-butylsilane: small silanes function essentially the same as donor ligands. Thus, a second equivalent of $Me_3SiH$ intercepts the unsaturated silyl complex $Cp_2Ta(SiMe_3)$ to produce $Cp_2Ta(H)(SiMe_3)_2$ (Scheme I) before alkylidene transfer from 1, rendering the reaction only stoichiometric in $Cp_2Ta(Me)$ rather than catalytic.[25] Formation of the analogous bis(silyl) complex from $H_2Si(t\text{-}Bu)_2$ is apparently prevented by unfavorable steric interactions.

**Reaction of $Cp_2Ta(=CH_2)(Me)$ with $H_2Si(t\text{-}Bu)_2$ in Benzene.** The reaction of 1 with $H_2Si(t\text{-}Bu)_2$ in benzene proceeds faster than in THF, and the phenyl methylene complex 5 is formed in addition to 2 and 3. Both differences are consistent with the mechanism proposed in Scheme II for the reaction in THF. The slower rate in THF may simply reflect interference by the coordinating solvent with either or both of the steps involving the unsaturated intermediates $Cp_2Ta(Me)$ (step 2) or $Cp_2Ta(SiH(t\text{-}Bu)_2)$ (step 4). In benzene these species will be essentially unsolvated; thus, associative processes should be faster.

The incorporation of benzene as a phenyl ligand in 5 is consistent with the intermediacy of the unsaturated silyl complex $Cp_2Ta(SiH(t\text{-}Bu)_2)$ in the reaction scheme. We

(19) For a general review, see: Tilley, T. D. In *The Chemistry of Organic Silicon Compounds*; Patai, S., Rappoport, Z., Eds.; Wiley: New York, 1989; Chapter 24, p 1415.

(20) (a) Randolf, C. L.; Wrighton, M. S. *J. Am. Chem. Soc.* **1986**, *108*, 3366. (b) Arnold, J.; Engeler, M. P.; Elsner, F. H.; Heyn, R. H.; Tilley, T. D. *Organometallics* **1989**, *8*, 2284.

(21) (a) Ingle, W. M.; Preti, G.; MacDiarmid, A. G. *J. Chem. Soc., Chem. Commun.* **1973**, 497. (b) Tilley, T. D. *J. Am. Chem. Soc.* **1985**, *107*, 4084.

(22) (a) Campion, B. K.; Falk, J.; Tilley, T. D. *J. Am. Chem. Soc.* **1987**, *109*, 2049. (b) Elsner, F. H.; Tilley, T. D.; Rheingold, A. L.; Geib, S. J. *J. Organomet. Chem.* **1988**, *358*, 169. (c) Campion, B. K.; Heyn, R. H.; Tilley, T. D. *J. Am. Chem. Soc.* **1990**, *112*, 2011.

(23) (a) Pannell, K. H.; Cervantes, J.; Hernandez, C.; Vinceti, S. *Organometallics* **1986**, *5*, 1056. (b) Berryhill, S. R.; Clevenger, G. L.; Burdurli, P. Y. *Organometallics* **1984**, *4*, 1509. (c) Crocco, G. L.; Young, C. S.; Lee, K. E.; Gladysz, J. A. *Organometallics* **1988**, *7*, 2158. (d) Schubert, U.; Schenkel, A. *Chem. Ber.* **1988**, *121*, 939.

(24) Parkin, G.; Bunel, E.; Burger, B. J.; Trimmer, M. S.; van Asselt, A.; Bercaw, J. E. *J. Mol. Catal.* **1987**, *41*, 21.

(25) In theory, reaction of 1 with small silanes could proceed by a chain reaction with sufficiently low silane concentrations. This has not been directly observed, but we note that at high temperatures reaction of $Me_3SiH$ with 1 yields some $Me_4Si$ in addition to the bis(silyl) and methane. $Me_4Si$ could reasonably arise from a related alkylidene transfer process, if $Me_3SiH$ then intercepts the silyl-substituted alkyl $Cp_2Ta(CH_2SiMe_3)$. $Me_4Si$ formation has also been observed in the photolytic reaction of 1 with $Me_3SiH$: Hostetler, M. J.; Bergman, R. G., private communication.

**Scheme III**

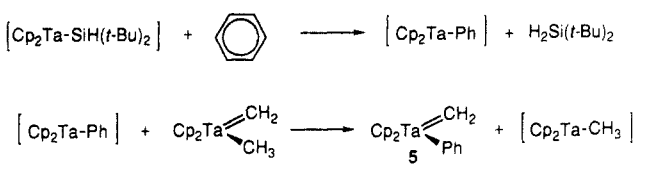

have previously shown that $Cp_2Ta(SiH(t\text{-}Bu)_2)(PMe_3)$ reacts with benzene under mild conditions, yielding the phenyl complex $Cp_2Ta(Ph)(PMe_3)$ and $H_2Si(t\text{-}Bu)_2$ (eq 17).[8] The reaction is strongly inhibited by added $PMe_3$, indicating that phosphine dissociation to yield $Cp_2Ta(SiH(t\text{-}Bu)_2)$ is necessary for the reaction to proceed.

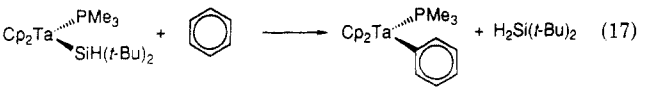

In the reaction of 1 with $H_2Si(t\text{-}Bu)_2$ in benzene, $Cp_2Ta(SiH(t\text{-}Bu)_2)$ is produced in the absence of trapping ligands and thus can rapidly react with benzene to generate an unsaturated phenyl species, $Cp_2Ta(Ph)$. Binuclear methylene transfer from 1 to $Cp_2Ta(Ph)$ would then yield 5 and regenerate $Cp_2Ta(Me)$, maintaining the catalytic cycle (Scheme III). As described above, the stoichiometric reaction of $Cp_2Ta(Ph)(PMe_3)$ with 1 does indeed produce 5 (eq 11). In this instance, however, $Cp_2Ta(Me)$ is trapped by the stoichiometric quantity of phosphine present.

**Relative Rates of Ligand-to-Alkylidene Migration in $Cp_2Ta(=CHR)(X)$.** A qualitative ranking of the rates of ligand-to-alkylidene migration in complexes of the type $Cp_2Ta(=CHR)(X)$ (X = H, $SiH(t\text{-}Bu)_2$, Ph, Me) is possible from an examination of several of the reactions described above. Not surprisingly, hydride exhibits the fastest rate of migration, demonstrated by the rapid transformation of 2 into 4, even at low temperatures (eq 3). The silyl ligand (X = $SiH(t\text{-}Bu)_2$, 7) also migrates readily, with a half-life of minutes at −10 °C (eq 9). In contrast, phenyl migration requires ca. 5 h at 65 °C (eq 7). Finally, Schrock and Sharp reported that although methyl migration in 1 is not competitive with bimolecular disproportionation, methyl migration does occur over 24 h at 75 °C in the analogous ethylidene complex $Cp_2Ta(=CHMe)(Me)$.[13] Thus, the order of migratory aptitudes in the $Cp_2Ta(=CHR)(X)$ system is H > $SiH(t\text{-}Bu)_2$ ≫ Ph > Me.

Analogous alkylidene migratory insertions in $Cp^*_2Ta(R)(=CH_2)$ (R = H, Me) have been studied by Bercaw and co-workers, who found that hydride migration is ca. $10^8$ times faster than methyl migration.[24] However, phenyl migration is not observed in $Cp^*_2Ta(=CH_2)(Ph)$.[26] The relatively facile formation of 6 from $Cp_2Ta(=CH_2)(Ph)$ may result from the necessary alignment of the p orbital on the phenyl ipso carbon with the $\pi$ system of the methylene ligand prior to migration, a configuration that would orient the phenyl ortho hydrogens toward the Cp ligands and that would be extremely unfavorable in the bulky bis(pentamethylcyclopentadienyl) system.

Cooper and co-workers[27] have demonstrated that ligand-to-methylene migration is extremely facile in cationic tungstenocene systems $[Cp_2W(=CH_2)(R)]^+$ (R = H, alkyl, Ph). Although these complexes are isoelectronic and isostructural with the tantalum complexes described above, the cationic charge renders the tungsten complexes significantly more electrophilic, leading apparently to an increase in the migration rates by several orders of magnitude.

The intramolecular migration of niobium hydride and alkyl ligands onto the oxygen-substituted carbene center in $Cp_2Nb(R)(=CHOR')$ (R' = $Cp^*_2ZrH$) was also examined by Threlkel and Bercaw,[28] who determined the order of migratory aptitudes to be H ≫ Me > $CH_2C_6H_4OCH_3$ > $CH_2Ph$. Phenyl group migration was not observed in this system up to 80 °C. The lack of mobility of the phenyl group is somewhat surprising, as the $Cp_2Nb$ center is only slightly more sterically congested at the metal than 5. It is possible that the phenyl migration is inhibited by the electrophilic nature of the oxycarbene. It has been suggested that migrations to electrophilic carbenes parallel those to metal carbonyls,[27,28] and Casey has shown that migratory insertion in rhenium carbonyl complexes is substantially slower for phenyl than for methyl.[29] Nonetheless, phenyl migration to the electrophilic carbene in $[Cp_2W(=CH_2)(Ph)]^+$ is quite rapid (10 min at room temperature),[27b] and thus, the lack of reactivity of $Cp_2Nb(Ph)(=CHOR')$ must be viewed as anomalous.

## Experimental Section

**General Considerations.** All manipulations were carried out under dry nitrogen with high vacuum line or Schlenk techniques or in a Vacuum Atmospheres drybox. Glassware was oven dried before use. Petroleum ether (boiling range 35–65 °C), tetrahydrofuran (THF), benzene, and toluene were freshly distilled from sodium/benzophenone ketyl. The following compounds were prepared by literature methods: $Cp_2Ta(CH_2)(CH_3)$,[13] $Cp_2Ta(C_6H_5)(PMe_3)$,[8] $Cp_2Ta(Si(t\text{-}Bu)_2H)(PMe_3)$,[8] $CpCp'Ta(CH_2)(CH_3)$,[13] $CpCp'Ta(PMe_3)(CH_3)$,[13] and $Me_3P{=}CH_2$.[30] $H_2Si(t\text{-}Bu)_2$ was obtained from Lithium Corporation of America, dried over molecular sieves, and degassed prior to use. Photochemical reactions were carried out in a Rayonet photochemical reactor with low-pressure mercury arc lamps (350 nm). Infrared spectra were measured on a Perkin-Elmer 1430 spectrophotometer. Routine $^1H$ NMR spectra were obtained by using IBM-Bruker AC 250 or AM 200 spectrometers. $^{13}C$ NMR experiments were performed on a IBM-Bruker AM 500 spectrometer using the DEPT or INEPT pulse sequences or gated coupled spectra to obtain coupling constants. Kinetics experiments were run with sealed NMR tubes in the thermostated probe of the spectrometer, and the temperature was calibrated with a methanol standard. Concentrations were determined from the integrated intensities of the Cp resonances vs hexamethylbenzene internal standard. Plots of $[1]^{-1}$ vs time were fit by using a linear least-squares regression, and in all cases $R \geq 0.998$. Elemental analyses were performed by Desert Analytics, Galbraith Laboratories, or Mikroanalytisches Labor Pascher (Germany). High-resolution mass spectral analyses were performed on a VG Instruments ZAB-E spectrometer.

**Formation of $Cp_2Ta(H)(=CHSiH(t\text{-}Bu)_2)$ (2) in THF.** Twelve milligrams (0.04 mmol) of 1, 25 μL (0.14 mmol) of $(t\text{-}Bu)_2SiH_2$, and 0.3 mL of THF-$d_8$ were added to an NMR tube which was subsequently sealed under nitrogen. After 3 days at room temperature, $^1H$ NMR spectroscopy showed formation of 2 and 3 (ca. 4:1). $^1H$ NMR (250 MHz, THF-$d_8$): δ 10.50 (d, $^3J_{H\text{-}H}$ = 7.3 Hz, 1 H, =C*H*), 5.61 (s, 5 H, Cp), 5.56 (s, 5 H, Cp), 4.03 (d, $^3J_{H\text{-}H}$ = 7.3 Hz, 1 H, SiH), 1.39 (s, br, 1 H, TaH), 0.93 (s, 9 H, C$Me_3$), 0.85 (s, 9 H, C$Me_3$). $^{13}C$ NMR (125 MHz, THF-$d_8$): δ 234.8 ($^1J_{C\text{-}H}$ = 126.7 Hz, =CH), 97.1 (Cp), 96.3 (Cp), 29.1 (C$Me_3$), 18.2 (C$Me_3$), 16.9 (C$Me_3$). $^{29}Si$ (DEPT) (40 MHz, THF-$d_8$): δ 12.4.

**Preparation of $[CpTa(\mu_2\text{-}\eta^1\text{:}\eta^5\text{-}C_5H_4)]_2(\mu\text{-}C(H)(SiH(t\text{-}Bu)_2))$ (3).** The following procedure was used to obtain analytically pure 3. A solution of 110 mg (0.21 mmol) of $Cp_2Ta(Si(t\text{-}Bu)_2H)(PMe_3)$ and 225 mg (0.66 mmol) of $Cp_2Ta(CH_2)(CH_3)$ in 10 mL of THF was stirred at 65 °C for 3 h. Volatiles were removed under vacuum and the solids extracted with petroleum ether. The petroleum

(26) Trimmer, M. S.; Bercaw, J. E., private communication. Trimmer, M. S. Ph.D. Thesis, CIT, 1989.
(27) (a) Hayes, J. C.; Jernakoff, P.; Miller, G. A.; Cooper, N. J. *Pure Appl. Chem.* **1984**, *56*, 25. (b) Jernakoff, P.; Cooper, N. J. *Organometallics* **1986**, *5*, 747.
(28) Threlkel, R. S.; Bercaw, J. E. *J. Am. Chem. Soc.* **1981**, *103*, 2650.
(29) Casey, C. P.; Scheck, D. M. *J. Am. Chem. Soc.* **1980**, *102*, 2723.
(30) Schmidbauer, H. *Inorg. Synth.* **1989**, *18*, 135.

ether was removed under vacuum, and the resulting solids were sublimed at 60 °C overnight to remove $Cp_2Ta(C_2H_4)(CH_3)$ and $Cp_2Ta(PMe_3)(CH_3)$. The residue was dissolved in 5 mL of toluene and passed through a 1-in. pad of neutral alumina on a medium-porosity sintered glass frit. The pad was washed with 5 mL of petroleum ether, and the resulting solution was stripped in vacuo to yield 140 mg (0.18 mmol) of dark blue microcrystalline product (86% yield based on $Cp_2Ta(Si(t\text{-}Bu)_2H)(PMe_3)$). Several of the proton and carbon resonances of the two inequivalent $C_5H_4$ rings in **3** overlap in the respective one-dimensional spectra, but all chemical shifts could be assigned on the basis of a two-dimensional COSY spectrum. $^1H$ NMR (250 MHz, $C_6D_6$): δ 5.43 (s, 5 H, Cp), 5.42 (s, 5 H, Cp), 4.71 (m, 2 H, $C_5H_4$), 4.67 (d, $^3J_{H\text{-}H}$ = 2.9 Hz, 1 H, Si*H*), 4.58 (m, 2 H, $C_5H_4$), 4.50 (m, 2 H, $C_5H_4$), 4.39 (m, 2 H, $C_5H_4$), 2.62 (d, $^3J_{H\text{-}H}$ = 2.9 Hz, 1 H, μ-C*H*), 1.24 (s, 18 H, C$Me_3$). $^{13}C$ NMR (125 MHz, $C_6D_6$): δ 157.0 ($C_5H_4$, μ-C), 150.6 ($C_5H_4$, μ-C), 127.9 ($C_5H_4$), 118.4 ($C_5H_4$), 107.3 ($C_5H_4$), 107.2 ($C_5H_4$), 99.4 (μ-CH), 98.9 ($C_5H_4$), 98.8 ($C_5H_4$), 98.3 (Cp), 98.2 ($C_5H_4$), 98.1 ($C_5H_4$), 98.0 (Cp), 31.7 (C$Me_3$), 31.7 (C$Me_3$), 23.9 (C$Me_3$), 22.6 (C$Me_3$). $^{29}Si$ (DEPT) (40 MHz, $C_6D_6$): δ 28.0. Anal. Calcd for $C_{29}H_{38}SiTa_2$: C, 44.85; H, 4.93. Found: C, 44.39; H, 4.91.

**Preparation of $Cp_2Ta(CH_2SiH(t\text{-}Bu)_2)(CO)$ (4a).** A solution of 300 mg (0.88 mmol) of $Cp_2Ta(CH_2)(CH_3)$ and 2.0 mL (11.1 mmol) of $(t\text{-}Bu)_2SiH_2$ in 15 mL of THF was heated to 65 °C for 1.5 h. Excess CO was then introduced at 25 °C, and the reaction mixture was stirred for 1 h. The volatiles were removed under vacuum to yield an oily solid. Residual silane was removed by trituration with petroleum ether followed by removal of volatiles under vacuum. Sublimation at 85 °C and $10^{-3}$ Torr yielded 270 mg (0.54 mmol) of green microcrystalline product (62% yield). $^1H$ NMR (250 MHz, $C_6D_6$): δ 4.50 (s, 10 H, Cp), 3.81 (t, $^3J_{H\text{-}H}$ = 2.7 Hz, 1 H, SiH), 1.25 (s, 18 H, C$Me_3$), -1.37 (d, $^3J_{H\text{-}H}$ = 2.7 Hz, 2 H, $CH_2$). $^{13}C$ NMR (125 MHz, $C_6D_6$): δ 263.8 (*C*≡O), 90.5 (Cp), 30.2 (C$Me_3$), 19.9 (C$Me_3$), -37.9 ($CH_2$). $^{29}Si$ (DEPT) (40 MHz, $C_6D_6$): δ 24.8. IR (Nujol mull): 1894 (ν(CO)), 2052 $cm^{-1}$ (ν(SiH)). Anal. Calcd for $C_{20}H_{31}OSiTa$: C, 48.38; H, 6.29. Found: C, 48.23; H, 6.44.

**Formation of $Cp_2Ta(PMe_3)(CH_2SiH(t\text{-}Bu)_2)$ (4b).** To a benzene solution containing a 70:30 mixture of **2** and **3** (25 mg) was added $PMe_3$ (0.12 mmol). $^1H$ NMR spectrum obtained after 10 min at room temperature showed complete conversion of **2** to **4b**. Compound **3** was left unchanged. Removal of the volatiles in vacuo led to the regeneration of the original 70:30 mixture of **2** and **3**. $^1H$ NMR (250 MHz, $C_6D_6$): δ 4.35 (d, $J_{P\text{-}H}$ = 1.8 Hz, 10 H, Cp), 3.83 (t, $J_{H\text{-}H}$ = 3.4 Hz, 1 H, SiH), 1.22 (s, 18 H, C$Me_3$), 0.85 (d, $J_{P\text{-}H}$ = 6.9 Hz, 9 H, P$Me_3$), -1.53 (d of d, $J_{H\text{-}H}$ = 3.4, $J_{P\text{-}H}$ = 6.4 Hz, 2 H, C$H_2$). $^{13}C$ NMR (125 MHz, $C_6D_6$): δ 85.5 (Cp), 30.4 (C$Me_3$), 28.6 (C$Me_3$), 19.3 ($J_{P\text{-}C}$ = 23.4 Hz, P$Me_3$), -49.5 ($J_{P\text{-}C}$ = 8.7, $J_{C\text{-}H}$ = 107.8 Hz, $CH_2$).

**Preparation of $Cp_2Ta(CH_2)(C_6H_5)$ (5a).** A solution of 200 mg (0.43 mmol) of $Cp_2Ta(PMe_3)(C_6H_5)$ and 0.250 mL (2.19 mmol) of $Me_3P{=}CH_2$ in 20 mL of THF was photolyzed at 0 °C for 15 h. The solvent and excess $Me_3P{=}CH_2$ were removed under vacuum, and the resulting solids were extracted with petroleum ether (50 mL), leaving a substantial quantity of brown residue. This material was soluble in toluene but exhibited no resonances in the $^1H$ NMR spectrum and thus may be paramagnetic. Recrystallization of the original filtrate from petroleum ether at -78 °C yielded 65 mg (0.16 mmol) of silvery-white crystals (38% yield). $^1H$ NMR (250 MHz, $C_6D_6$): δ 10.64 (s, 2 H, =C$H_2$), 7.56 (m, 2 H, $C_6H_5$), 7.08 (m, 3 H, $C_6H_5$), 5.11 (s, 10 H, Cp). $^{13}C$ NMR (125 MHz, $C_6D_6$): δ 239.1 ($^1J_{C\text{-}H}$ = 132.3 Hz, =$CH_2$), 166.3 ($C_6H_5$), 149.4 ($C_6H_5$), 126.5 ($C_6H_5$), 122.9 ($C_6H_5$), 100.1 (Cp). High-resolution MS (*m/e*): calcd, 402.081; found, 402.087. Satisfactory elemental analysis could not be obtained, possibly due to contamination with the brown complex, despite multiple recrystallizations.

**Reaction of 1 with $(t\text{-}Bu)_2SiH_2$ in Benzene.** Fifteen milligrams (0.04 mmol) of **1**, 40 μL (0.22 mmol) of $(t\text{-}Bu)_2SiH_2$, and 0.3 mL of benzene-$d_6$ were added to an NMR tube which was subsequently sealed under nitrogen. After 6 h at 25 °C, the $^1H$ NMR spectra showed formation of **2**, **3**, and **5** (ca. 1.9:1:2.3). $^1H$ NMR of $Cp_2TaH(=CH(Si(t\text{-}Bu)_2H)$ (**2**) ($C_6D_6$): δ 10.72 (d, $^3J_{H\text{-}H}$ = 7.3 Hz, 1 H, =CH), 5.27 (s, 5 H, Cp), 5.05 (s, 5 H, Cp), 4.67 (d, $^3J_{H\text{-}H}$ = 7.3 Hz, 1 H, SiH), 1.56 (s, br, 1H, TaH), 1.18 (s, 9 H, $CMe_3$), 1.17 (s, 9 H, $CMe_3$).

**Reaction of 1 with $Me_3SiH$ in THF.** $Me_3SiH$ (0.147 mmol) was condensed at -196 °C onto a frozen solution of 10 mg (0.029 mmol) of **1** in 0.3 mL of THF-$d_8$ in an NMR tube, and the tube was sealed under vacuum. After ca. 30 days at 25 °C or 2 days at 65 °C, the $^1H$ NMR spectra showed complete conversion of **1** to $Cp_2Ta(H_2C{=}CH_2)(CH_3)$, $Cp_2Ta(SiMe_3)_2H$, and methane.

**Formation of $Cp_2Ta(PMe_3)(CH_2Ph)$ (6).** Ten milligrams (0.025 mmol) of **5**, 12 μL (0.125 mmol) of $PMe_3$, and 0.3 mL of benzene-$d_6$ were sealed in an NMR tube under nitrogen. The tube was heated at 65 °C for 5 h at which time the $^1H$ NMR spectrum showed complete conversion of **5** to **6**. $^1H$ NMR of $Cp_2Ta(PMe_3)(CH_2Ph)$ (**6**) (250 MHz, $C_6D_6$): δ 7.28 (m, 2 H, $C_6H_5$), 7.05 (m, 3 H, $C_6H_5$), 4.21 (d, $J_{P\text{-}H}$ = 1.8 Hz, 10 H, Cp), 1.67 (d, $J_{P\text{-}H}$ = 4.8 Hz, 2 H, C$H_2$Ph), 0.81 (d, $J_{P\text{-}H}$ = 7.0 Hz, 9 H, P$Me_3$). $^{13}C$ NMR (125 MHz, $C_6D_6$): δ 149.5 ($C_6H_5$), 129.1 ($C_6H_5$), 127.5 ($C_6H_5$), 126.7 ($C_6H_5$), 86.3 (Cp), 20.1 (d, $J_{P\text{-}C}$ = 23.4 Hz, $J_{C\text{-}H}$ = 128.2, P$Me_3$), 0.3 ($J_{C\text{-}H}$ = 120.5 Hz, $CH_2$).

**Formation and Observation of 7 at Low Temperatures.** $Cp_2Ta(Si(t\text{-}Bu)_2H)(PMe_3)$ (10 mg, 0.019 mmol), $Me_3P{=}CH_2$ (4 μL, 0.035 mmol), and THF-$d_8$ (0.3 mL) were sealed in an NMR tube under nitrogen. The solution was photolyzed at -70 °C for 5 h. The NMR tube was then transferred to the cooled probe of the spectrometer. $^1H$ NMR spectra observed at -70 °C showed 66% conversion to **7**. The temperature was gradually raised, and at -20 °C the Cp resonances of **7** were observed to be in coalescence. A small amount of **4b** was also observed. Conversion to **4b** was complete after 30 min at -10 °C. $^1H$ NMR of $Cp_2Ta(=CH_2)(SiH(t\text{-}Bu)_2)$ at -70 °C: δ 10.44 (AB quartet, 2 H, Ta=C$H_2$), 5.61 (s, 5 H, Cp), 5.43 (s, 5 H, Cp), 4.01 (s, 1 H, Si*H*), 1.34 (s, 9 H, $CMe_3$), 1.32 (s, 9 H, $CMe_3$).

**Crossover Reaction between 1 and $CpCp'Ta(CH_3)(PMe_3)$.** Ten milligrams (0.029 mmol) of **1**, 12 mg (0.029 mmol) of $CpCp'Ta(CH_3)(PMe_3)$, and 0.3 mL of benzene-$d_6$ were sealed in an NMR tube under nitrogen. The reaction was periodically monitored by $^1H$ NMR spectroscopy. A statistical mixture of **1**, $CpCp'Ta(CH_3)(PMe_3)$, $Cp_2Ta(CH_3)(PMe_3)$, and $CpCp'Ta(CH_3)(=CH_2)$ was reached after 51 h at 25 °C. Approximately 5% $Cp_2Ta(C_2H_4)(Me)$ and $CpCp'Ta(C_2H_4)(Me)$ was also observed. The components of the mixture were confirmed by comparison of the $^1H$ NMR spectra to those of authentic samples. The same equilibrium mixture was obtained similarly starting with $Cp_2Ta(CH_3)(PMe_3)$ and $CpCp'Ta(CH_3)(=CH_2)$.

**Reaction of $Cp_2Ta(C_6H_5)(PMe_3)$ with 1.** Five milligrams (0.015 mmol) of **1** and 7 mg (0.015 mmol) of $Cp_2Ta(C_6H_5)(PMe_3)$ in 0.3 mL benzene-$d_6$ were sealed in an NMR tube under nitrogen. After 10 days at 25 °C, the $^1H$ NMR spectra showed ca. 60% conversion of $Cp_2Ta(C_6H_5)(PMe_3)$ to $Cp_2Ta(CH_3)(PMe_3)$ and **5**.

**Reaction of $Cp_2Ta(Si(t\text{-}Bu)_2H)(PMe_3)$ with 1.** Six milligrams (0.018 mmol) of **1**, 9 mg (0.017 mmol) of $Cp_2Ta(Si(t\text{-}Bu)_2H)(PMe_3)$, and 0.3 mL of THF-$d_8$ were sealed in an NMR tube under vacuum. After 4 weeks at 25 °C, the $^1H$ NMR spectrum showed a mixture of **2**, **3**, **4b**, and $Cp_2Ta(CH_3)(PMe_3)$ (1:3.3:1.8:6.5).

**Crystallographic Procedures for 3 and 4a.** Single crystals of suitable size were sealed in 0.5-mm thin-walled Pyrex capillaries in a glovebox, and the capillaries were mounted on the diffractometer. Refined cell dimensions and their standard deviations were obtained from least-squares refinement of 25 accurately centered reflections with $2\theta > 25°$. Crystal data are summarized in Table I.

Diffraction data were collected at 295 K on an Enraf-Nonius four-circle CAD-4 diffractometer employing Mo Kα radiation filtered through a highly oriented graphite crystal monochromator. The intensities of three standard reflections measured at intervals of ca. 80 reflections showed no systematic change during data collection. Data collection is summarized in Table I. The raw intensities were corrected for Lorentz and polarization effects by using the program BEGIN from the SDP+ package.[31] Empirical absorption corrections based on ψ scans were also applied.

All calculations were performed on a VAX 11/785 computer using the SDP+ software package.[31] The full-matrix least-squares refinement was based on *F*, and the function minimized was $\sum w(|F_o| - |F_c|)^2$. The weights (*w*) were taken as $4F_o^2/(\sigma(F_o^2))^2$

(31) B. A. Frenz and Associates, Inc., College Station, TX 77840, and Enraf-Nonius, Delft, Holland.

where $|F_o|$ and $|F_c|$ are the observed and calculated structure factor amplitudes. Atomic scattering factors and complex anomalous dispersion corrections were taken from refs 32-34. Agreement factors are defined as $R_1 = \sum||F_o| - |F_c||/\sum|F_o|$ and $R_2 = [\sum w||F_o| - |F_c||^2/\sum w|F_o|^2]^{1/2}$. The goodness-of-fit is defined as GOF = $[\sum w(|F_o| - |F_c|)^2/(N_o - N_p)]^{1/2}$, where $N_o$ and $N_p$ are the number of observations and parameters.

The coordinates of the tantalum and silicon atoms were obtained from three-dimensional Patterson maps. Analysis of subsequent difference Fourier maps led to the location of the remaining heavy atoms. Refinement using anisotropic Gaussian amplitudes followed by difference Fourier synthesis resulted in the location of the silicon hydrogens, most of the Cp hydrogens, and at least one hydrogen on each methyl group. All remaining hydrogen atoms were placed at idealized locations ($D$(C-H) = 0.95 Å) by using the program HYDRO.[31] Final refinement included anisotropic Gaussian amplitudes for all non-hydrogen atoms and fixed positions and fixed isotropic parameters for the hydrogen atoms. Final agreement factors are listed in Table I. Final positional parameters, Gaussian amplitudes, and structure factor amplitudes for **3** and **4a** are included in the supplementary material.

**Acknowledgment.** Financial support of this work by the National Science Foundation (Grant CHE-8808161) is gratefully acknowledged. We are also grateful to Dr. Terry Rathman of the Lithium Corporation of America for a generous gift of silanes. D.H.B. also thanks the University of Pennsylvania Natural Science Association for a Young Faculty Award.

**Supplementary Material Available:** Tables of positional parameters and their estimated standard deviations, anisotropic thermal parameters, and intramolecular distances and angles (16 pages); tables of final structure factor amplitudes for **3** and **4a** (36 pages). Ordering information is given on any current masthead page.

(32) *International Tables for X-Ray Crystallography*; Kynoch: Birmingham, England, 1974; Vol. IV, Table 2.2B.
(33) Stewart, R. F.; Davidson, E. R.; Simpson, W. T. *J. Chem. Phys.* **1965**, *42*, 3175-3187.
(34) *International Tables for X-Ray Crystallography*; Kynoch: Birmingham, England, 1974; Vol. IV, Table 2.3.1.

# Open and Half-Open Ruthenocenes and Osmocenes: Protonations, Structures, and Reactions with Carbonyl and Phosphine Ligands

Timothy D. Newbound,[1] Lothar Stahl,[1] Manfred L. Ziegler,*[,2] and Richard D. Ernst*[,1]

*Department of Chemistry, University of Utah, Salt Lake City, Utah 84112, and Institut für Anorganische Chemie der Universität Heidelberg, D-6900 Heidelberg 1, West Germany*

*Received March 22, 1990*

The synthesis of a protonated "open ruthenocene", "$HRu(2,4\text{-}C_7H_{11})_2{}^+BF_4{}^-$", is reported, as well as its osmium analogue. The addition of 1 equiv of CO or $P(OMe)_3$ leads to the formation of mono(ligand) adducts, during which one of the pentadienyl ligands and the hydride ligand combine to yield an $\eta^4$-2,4-dimethylpentadiene complex, in accord with the formulation of "$HRu(2,4\text{-}C_7H_{11})_2{}^+$" as an agostic species. The addition of 2 equiv of a second ligand to the monoadducts then brings about the removal of the diene ligand, allowing isolation of $Ru(2,4\text{-}C_7H_{11})(CO)_2(PEt_3)^+$ and $Ru(2,4\text{-}C_7H_{11})(CO)(PEt_3)_2{}^+$, as well as symmetric complexes such as $Ru(2,4\text{-}C_7H_{11})(L)_3{}^+$ (L = CO, $P(OMe)_3$, $PMe_3$). X-ray diffraction studies are reported for several of these compounds. Crystals of $Os(C_5H_5)(2,4\text{-}C_7H_{11})$ are isomorphous with the iron and ruthenium analogues, being orthorhombic, space group *Pnma* (No. 62), with $a$ = 5.900 (2) Å, $b$ = 13.089 (7) Å, $c$ = 13.503 (6) Å, and $Z$ = 4. The structure was refined to discrepancy indices of $R$ = 0.043 and $R_W$ = 0.044 for 1170 reflections having $I > 2.5\sigma(I)$ and revealed similar Os-C distances for the open and closed dienyl ligands. Crystals of $Ru(2,4\text{-}C_7H_{11})(\eta^4\text{-}2,4\text{-}C_7H_{12})(CO)^+BF_4{}^-$ are monoclinic, space group $P2_1/n$ (No. 14), with $a$ = 8.436 (6) Å, $b$ = 13.818 (4) Å, $c$ = 15.199 (9) Å, $\beta$ = 104.72 (5)°, and $Z$ = 4. The structure was refined to discrepancy indices of $R$ = 0.053 and $R_W$ = 0.046 for 2337 reflections having $I > 2.5\sigma(I)$. The general structure involves the diene and dienyl fragments having their open edges essentially eclipsed, with the carbonyl ligand being situated between these open edges. Crystals of $Ru(2,4\text{-}C_7H_{11})(CO)_2(PEt_3)^+BF_4{}^-$ are monoclinic, space group $P2_1/m$ (No. 11), with $a$ = 8.863 (2) Å, $b$ = 12.246 (2) Å, $c$ = 9.801 (2) Å, $\beta$ = 112.98 (2)°, and $Z$ = 2. The structure was refined to discrepancy indices of $R$ = 0.037 and $R_W$ = 0.032 for 2337 reflections having $I > 2.5\sigma(I)$. The structure may be regarded as symmetric, with the phosphine ligand located under the open edge of the dienyl ligand and the two carbonyl ligands located under the formally uncharged pentadienyl carbon atoms in the 2- and 4-positions. The carbonyl ligands are crystallographically equivalent, being related to one another by a mirror plane that bisects the dienyl and phosphine ligands. Crystals of $Ru(2,4\text{-}C_7H_{11})(CO)(PEt_3)_2{}^+BF_4{}^-$, as an apparent ethanol solvate, are monoclinic, space group $P2_1/n$ (No. 14), with $a$ = 10.809 (3) Å, $b$ = 27.134 (7) Å, $c$ = 10.879 (3) Å, $\beta$ = 115.40 (2)°, and $Z$ = 4. The structure was refined to discrepancy indices of $R$ = 0.067 and $R_W$ = 0.054 for 1578 reflections having $I > 2.5\sigma(I)$. This structure may be regarded as unsymmetric, being related to the previous one by replacement of one carbonyl ligand under a formally uncharged carbon atom by the second $PEt_3$ molecule.

Pentadienyl ligands have recently been attracting growing attention.[3] To a large extent, this has occurred as a result of pentadienyl's ability to bond to transition metals very favorably, in some cases better than cyclo-

(1) University of Utah.
(2) Universität Heidelberg.

0276-7333/90/2309-2962$02.50/0 